ResearchGate

See discussions, stats, and author profiles for this publication at: https://www.researchgate.net/publication/235442697

Decreasing the diabetic complication by vanadyl(VO)2+/vitamin B6 complex in alloxan-induced diabetic mice

ARTICLE *in* JOURNAL OF MATERIALS SCIENCE MATERIALS IN MEDICINE · FEBRUARY 2013

Impact Factor: 2.59 · DOI: 10.1007/s10856-013-4852-2 · Source: PubMed

CITATIONS
3

READS
75

3 AUTHORS, INCLUDING:

Nahla S. El-Shenawy
Taif University . saudi Arabia. and Suez can…

57 PUBLICATIONS **427** CITATIONS

SEE PROFILE

Available from: Nahla S. El-Shenawy
Retrieved on: 02 February 2016

J Mater Sci: Mater Med (2013) 24:911–930
DOI 10.1007/s10856-013-4852-2

Decreasing the diabetic complication by vanadyl$(VO)^{2+}$/vitamin B_6 complex in alloxan-induced diabetic mice

Nahla S. El-Shenawy · Moamen S. Refat · Fatima H. Fakihi

Received: 9 October 2012 / Accepted: 16 January 2013 / Published online: 9 February 2013
© Springer Science+Business Media New York 2013

Abstract The scope of this work was to synthesize a novel bifunctionalized vanadyl$(VO)^{2+}$/vitamin B_6 complex. The diabetic therapeutic efficacy of the new complex was investigated in alloxan-induced diabetic mice. The results suggested that vanadyl$(VO)^{2+}$/vit B6 complex has an anti-diabetic potency, improved the lipid profile and liver and kidney functions. The new complex possesses an antioxidant activity. The current results support the therapeutic potentiality of vanadyl$(VO)^{2+}$/vitamin B_6 complex for the management of diabetes.

1 Introduction

Diabetes mellitus (DM) is a disease that is increasingly affecting millions of people all over the world. Currently, there are over 150 millions diabetics worldwide and this is likely to increase to 300 million or more by 2025 [1]. Diabetes is a chronic disorder affecting the population on epidemic level. Diabetes results from abnormal metabolism of insulin wherein insulin action is impaired or absolute insulin deficiency results in imbalance of glucose metabolism and leads to a syndrome called DM [2–4]. Abnormally elevated blood glucose level causes oxidative stress and the formation of advanced oxidation end products which results in diabetic complications [5]. In particular, diabetics are at increased risk for several types of kidney disease and disorder diabetic nephropathy [6]. However, clinical trials suggested that there is no effective treatment for diabetic nephropathy without undesirable side-effects or contraindications. Diabetes mellitus type 2 (DMT2) is characterized by tissue resistance to the action of insulin combined with a relative deficiency in insulin secretion. Although patients with insulin resistance still produce insulin in their beta cells, the secretion is inadequate and the blood glucose level increases [7]. In DMT2, insulin resistance in the liver reflects the failure of hyperinsulinemia to suppress gluconeogenesis, resulting in fasting hyperglycemia and decreased liver glycogen storage in the postprandial state. Gluconeogenesis is important in preventing an excessive reduction in the blood glucose concentration during fasting [8]. The liver plays a key role in maintaining blood glucose levels during fasting by converting its stored glycogen into glucose (glycogenolysis) and by synthesizing glucose, mainly from lactate and amino acids (gluconeogenesis) [8].

Numerous in vitro and in vivo studies show that vanadium has insulin-like effects in the liver, skeletal muscle and adipose tissue [9–16]. Vanadium is not only an important trace element for organisms, but also the necessary element for human body [10]. It has been demonstrated that many vanadium compounds possess therapeutic effects as insulin mimetic [11]. Vanadium compounds are relatively well known both as free oxygen radicals generators in some inorganic and bio-reaction mechanisms and

N. S. El-Shenawy · F. H. Fakihi
Biology Department, Faculty of Science, Taif University, Qurwa, Taif 888, Saudi Arabia

N. S. El-Shenawy (✉)
Zoology Department, Faculty of Science, Suez Canal University, Ismailia, Egypt
e-mail: elshenawy_nahla@hotmail.com

M. S. Refat (✉)
Department of Chemistry, Faculty of Science, Port Said University, Port Said, Egypt
e-mail: msrefat@yahoo.com

M. S. Refat
Department of Chemistry, Faculty of Science, Taif University, Taif 888, Saudi Arabia

as complex activators or inhibitors of many enzymes involved in carbohydrate or lipid metabolic pathways. Vanadium seems to increase insulin receptor substrate-1 phosphorylation, acting as an insulin-sensitizing agent [12]. Vanadium compounds, as a nonspecific phosphotyrosine phosphatase inhibitor, have been known to possess insulin mimetic and/or enhancing effects both in vitro and in vivo [13]. Several studies have shown that vanadium compounds improve not only hyperglycemia in human subjects and animal models of type-one diabetes but also glucose homeostasis in type 2 diabetes [3, 14–16]. Two inorganic vanadium salts, vanadyl sulfate and sodium metavanadate, have entered the phase I clinical trials, but further development is impeded by the lower bioavailability and greater irritation to digestive track. For vanadium to be useful as an orally available hypoglycemic agent, it must be able to cross biological membranes, both for the initial absorption process and for intracellular uptake. Most metal ions are assumed to cross cell membranes by passive diffusion, which requires that the metallo-complex (vanadium in a complex state) must have low molecular weight, no positive or negative charge, and a fair degree of resistance to hydrolysis. The lipophilicity of the complex must be balanced with its hydrophilicity [17]. Therefore, vanadium complexes with organic ligands are considered to be more active and less toxic than inorganic vanadium salts. A new Schiff base, H_4pydmedpt$^{2+}\cdot 2Cl^-$, derived from one of the forms of vitamin B(6) has been synthesized by condensation of pyridoxal hydrochloride with *N*,*N*-bis[3-aminopropyl]-methylamine and characterized by analytical and spectroscopic methods [18]. They found that the inhibitory effect of oxidovanadium(IV) Schiff base complex on % glucose uptake determined with isolated rat adipocyte cells lower than for V(IV)OSO_4 and of the same order of magnitude of other reported insulin enhancing vanadium compounds.

Studies have shown that serum levels of pyridoxine (vitamin B_6) are below normal in approximately one quarter of adult and pediatric patients with DM, and that most people with DM have lower levels than non DM subjects, even if not outside the Ref. [19]. A study of experimentally induced DM in rats suggests an increased need for vitamin B_6 in subjects with DM due to its involvement in metabolic reactions which are increased in these subjects [20]. As such, pyridoxine supplementation of patients with DM was shown to improve glucose tolerance in one study; pyridoxine administered did not only effect on blood glucose but also reduced the concentration of glycosylated hemoglobin (HbA1c). This finding suggests that vitamin B_6 inhibits the glycosylation of proteins and might therefore help prevent diabetic complications [21].

One of the aims of this research was directed toward the synthesis and characterization of neutral symmetrical oxovanadium $(VO)^{2+}$ complex. Then the effects of new vanadyl$(VO)^{2+}$/vitamin B_6 complex on preventing the complication of diabetic that induced by alloxan in mice have been evaluated. The microbial test was performed for the new complex against some kinds of bacteria and fungi.

2 Materials and methods

2.1 Chemicals

Alloxan monohydrate was purchased from Sigma Chemical Co, USA. Kits of high density lipoprotein-cholesterol (HDL-c), cholesterol, triglycerides, total protein, creatinine, uric acid, glucose-6-phosphate dehydrogenase (G6PD) and lactate dehydrogenises (LDH) were purchased from Stanbio Laboratory, USA. Reduced glutathione (GSH; 99.8 %) was obtained from Sigma Company. Glacial metaphosphoric acid, sodium citrate, potassium chloride (KCl), Thiobarbituric acid (TBA), trichloroacetic acid (TCA), ethylenediaminetetraacetic acid (EDTA), sodium carbonate, acetic acid, epinephrine, sodium acetate, 2,4,6-tri(Z-pyridy)-*S*(riazine, 99 %) (TPTZ) $FeCl_3\cdot_6H_2O$, HCl, 5,5 dithiobis-(2-nitrobenzoic acid (DTNB), dimethyl sulphoside (DMSO), potassium dihydrogenophosphate (KH_2PO_4), phosphoric acid, butanol, and sodium chloride (NaCl) of technical grade used in this study were supplied by Sigma Chemical Co. (St. Louis, MO, USA). Other chemicals were procured from SRL Pvt., Ltd., Mumbai, India. Pyridoxine hydrochloride (Vitamin B6 hydrochloride) was received from Koch-Light Laboratories Ltd (Coin brook Berks England). $VOSO_4\cdot 2H_2O$ was obtained from Aldrich Chemical Company.

2.2 Synthesis of vanadyl$(VO)^{2+}$/vitamin B_6 complex

A solution of $VOSO_4\cdot 2H_2O$ (1.0 g, 5 mmol) in doubly distilled water (10 mL) was added drop wise to a stirred solution of vitamin B_6 (2.06 g, 10 mmol) in ethanol (25 mL). The resulted brownish green solution was stirred for about 1 h with heating at 60 °C. After few minutes the color of solution changed to a deep brownish green feature. Addition of ammonia solution (5 % w/w) till pH = 8 the brownish green precipitate was formed. It was filtered off, washed with ethanol and dried under vacuum over $CaCl_2$. The vanadyl$(VO)^{2+}$ solid complex was produced in 2.20 g.

2.3 Determination of some chemical parameters for the vanadyl$(VO)^{2+}$/vitamin B6 complex

Elemental analysis carbon, hydrogen and nitrogen contents were determined at the Micro analytical Center in Cairo University [22]. The percentage of vanadium metal in vitamin B_6 complex form was determined gravimetrically

by the direct ignition of the $VOSO_4$/vit B_6 complex at 800 °C for 3 h till constant weight. The residual was weighted in the form of V_2O_5 as a stable oxide feature. To confirm the presence or absence of sulfate content in the vanadyl$(VO)^{2+}$ complex, the saturated solution of $BaCl_2$ was used as a precipitating agent [23]. The mid infrared spectra of the reactants and the resulted vanadyl$(VO)^{2+}$ complex were measured from KBr discs using a Genesis II FT IR spectrophotometer [16]. Molar conductance measurements in DMSO solvent at 25 °C for the vitamin B_6 and its vanadyl$(VO)^{2+}$ complex with concentration 1.0×10^{-3} mol/L were carried out using Jenway 4010 conductivity meter. Magnetic measurements were carried out on a Sherwood Scientific magnetic balance using Gouy method. Two very good solid calibrates are used: $Hg[Co(CNS)_4]$ and $[Ni(en)_3](S_2O_3)$. The solid reflectance spectra were performed on a Shimadzu 3101pc spectrophotometer. TGA was carried out on a Shimadzu thermogravimetric analyzer at a heating rate of 10 °C min^{-1} under nitrogen atmosphere. ESR spectrum of the vanadyl$(VO)^{2+}$ complex was obtained on a Joel JES-FE2XG ESR Spectrometer with frequency (9.44 GHz). The X-ray diffraction patterns (XRD) were obtained on a Rikagu diffractometer using Cu/Kα radiation [24]. SEM images were taken in JEOL-840 equipment, with an accelerating voltage of 15 kV [25].

2.4 Experimental animals design

Male MFI mice (weighing 25–30 g) were purchased from King Fahed Medical Research Center in Jeddah (Kingdom of Saudi Arabia). The animals were maintained in solid-bottom shoe box type polycarbonate cages with stainless steel wire-bar lids, using a wooden dust-free litter as a bedding material. Animals were located in air-conditioned room and were allowed free access to pellet diet and tap water for a week before starting the experiment. The European Community Directive (86/609/EEC) and National rules on animal care have been followed. Animals were randomly divided into four groups with 10 animals in each one as following:

Group I (saline control) was normal and injected intraperitoneally (i.p.) with 0.1 mL of saline every alternative day for 30 days.

Group II (control vanadyl$(VO)^{2+}$/vitamin B_6 group) was injected i.p. each alternative day by vanadyl$(VO)^{2+}$/vit B_6 complex (40 mg/kg). This dose was selected according to Hussain [16].

Group III (untreated diabetic; positive control) was injected i.p. by a single dose of alloxan (150 mg/kg body weight) [27].

Group IV was injected with alloxan (150 mg/kg body weight) and then injected i.p. each alternative day by vanadyl$(VO)^{2+}$/vit B_6 complex (40 mg/kg) [16]. The treatment was carried out for 30 days after 72 h from alloxan injection.

The diabetic state was assessed by measuring serum glucose concentration after 72 h of alloxan treatment. Mice exhibiting serum glucose levels above 210 mg/dL were selected for the experiment and included in the study. The negative and positive groups were done twice.

The animals were carefully monitored every day and weighed every week during the period of the study. Animals described as fasted were deprived of food for 18 h but allowed free access to drinking water. Blood samples were drawn at the end of study and the tissue of liver and kidney were collected.

2.5 Induction of diabetes

Alloxan (150 mg/kg body weight) was dissolved in saline and was kept in dark bottle to avoid decomposition. After 18 h of fasting [27], mice were injected i.p. with a single dose of freshly prepared alloxan solution.

It was suggested that hypoglycemia is severe in fasted mice treated with a diabetogenic agent [28].

2.6 Collection of blood and organs

Blood samples of the fasted mice were collected from the medial retro-orbital venous plexus immediately with capillary tubes (Micro Haematocrit Capillaries, Mucaps) under ether anesthesia [26]. About 3 mL of blood collected in two tubes from each animal, one with EDTA for the hematological assays, the second was allowed to clot for 30 min. Then, the blood was centrifuged at 3,000 rpm for 15 min to separate serum for different biochemical analyses.

The animals were then dissected under ether anesthesia and tissue samples (liver and kidney) were collected, washed with 1.15 % of KCl and 0.5 mM of ethylenediaminetetraacetic acid (EDTA) and preserved in −20 °C for subsequent biochemical analyses.

2.7 Hematological parameters

A complete blood count includes five major measurements were determined using cell counter (Sysmex, model KX21N). White blood cells (WBC) were measured in thousands per cubic milliliter of blood. Red blood cells (RBC) were measured in millions per cubic mil-limeter of blood. Hemoglobin (Hb) was measured in grams per deciliter (g/dL) of blood. The haematocrit value (PCV) is

the percentage of red blood cells in relation to total blood volume was also determined. Mean cell volume (MCV), mean cell haemoglobin (MCH) and mean cell haemoglobin concentration (MCHC) were also calculated. Platelets were measured in thousands per cubic millime-ter of blood.

2.8 Lipid profile

Triglycerides, cholesterol and high density lipoprotein-cholesterol (HDL-c) were determined using the commercial kits. Low density lipoprotein-cholesterol (LDL-c) levels were calculated by using the following formula of Muruganandan et al. [29]: LDL-c = total cholesterol—(HDL-c + triglycerides)/5. Volatile low density lipoprotein-cholesterol (VLDL-c) levels were calculated by using the following formula of Prakasam et al. [30]: VLDL-c = triglyceride/5. The risk ratio was calculation by dividing the total cholesterol by HDL-c. Atherogenic index was calculated by using the following formula of Muruganandan et al. [29]: Atherogenic index = (total cholesterol-HDL-c)/HDL-c.

2.9 Liver and kidney functions

The activities of G6PDH and LDH as well as level of creatinine and uric acid were determined using the commercial kits.

2.10 Assessment of lipid peroxidation as oxidative bioindicator in tissues

The thiobarbituric acid reactive substances (TBARS) levels as an index of malondialdehyde (MDA) production were measured by the method described by Ohkawa et al. [31]. MDA, an end product of lipid peroxidation reacts with TBA-TCA complex to form a colored complex at high temperature exhibiting an absorption maximum at 535 nm.

2.11 Determination of enzymatic and non-enzymatic antioxidants

The principle of SOD activity assay was based on the inhibition of nitro blue tetrazolium (NBT) reduction. Illumination of riboflavin in the presence of O_2 and electron donor like methionine generates superoxide anions and this has been used as the basis of assay of SOD. The reduction of NBT by superoxide radicals to blue colored formazan was followed at 480 nm [32].

Glutathione-S-transferase (GST) was determined according to the method of Habig et al. [33].

Reduced glutathione level (GSH) as non-enzymatic antioxidant was estimated based on the method of Beutler et al. [34] who reported that the 5,5′-dithiobis-(2-nitrobenzoic acid) is reduced by SH group to form 1 mol of 2-nitro-5-mercaptobenzoic acid per mole of SH.

Total antioxidant capacity of hepatocytes was determined using ferric reducing antioxidant power assay according to the method of Prieto et al. [35]. FRAP reagent (300 mM acetate buffer, pH 3.6, 10 mM 2,4,6-tri(Z-pyridy)-S(riazine, 99 %) (TPTZ) in 40 mM HCl and 20 mM $FeCl_3 \cdot 6H_2O$ in the ratio of 10:1:1 was prepared. 1.5 mL FRAP reagent was added to 50 µL of homogenated liver or kidney tissue and incubated at 37 °C for exactly 5 min. The change in absorbance was measured at 593 nm due to the formation of a blue colored Fe^{II}-tripyridyltriazine complex from the colorless oxidized Fe^{III} form by the action of electron donating antioxidants. The absorbance of the sample was read against reagent blank (1.5 mL FRAP reagent and 50 µL distilled water) at 593 nm. The data was expressed as percentage of the control value.

Colorimetric determination of the total protein based on the principle of Biuret reaction (copper salts in an alkaline medium). Protein in plasma or serum forms a blue colored complex when treated with cupric icons in alkaline solution. The intensity of the blue color is proportional to the protein concentration [36].

2.12 Statistical analysis

The results were evaluated using an unpaired *t* test and analysis of variance (ANOVA) using the SPSS version 17.0 software packages for statistical evaluation. Values were presented as mean ± S.E. (n = 8–10; each group). Pearson's correlation analysis was performed to investigate the relationship among the different biochemical parameters. The significant consider at $P \leq 0.05$.

Table 1 Analytical and physical data for pyridoxine HCl (vit B_6) and its vanadyl$(VO)^{2+}$ complex

Compounds Empirical formula (M. Wt.)	Color Yield (%)	Λm ($\Omega^{-1}cm^{-1}mol^{-1}$)	Elemental analysis (%) found (Calcd.)					
			C	H	N	O	Cl	M
Vit B6 [$C_8H_{12}ClNO_3$] (205.05)	White	27	46.73	5.88	6.81	23.34	17.24	–
[VO(vit $B_6)_2$]·$2H_2O$ (439.31) $C_{16}H_{24}N_2O_9V$	Green 76 %	23	43.24 (43.74)	5.48 (5.51)	6.21 (6.38)	33.74 (32.77)	–	11.33 (11.60)

Table 2 Assignments of the IR and Raman spectral bands (cm^{-1}) for vit B_6 free ligand and its vanadyl$(VO)^{2+}$ complex

Vit B6		VO(IV) complex		Assignments[a]
IR	Raman	IR	Raman	
3,326 vs	–	3266 vs,br	–	ν(OH); alcoholic
3,241 vs		—		ν(OH); phenolic
3093 m	3105 vw, 2977 m, 2936 m, 2903 w	2832 m, br	–	ν(CH); aromatic
2822 vs	2866 w, 2831 w			ν(CH); aliphatic
1996 vw	–	2074 w, br	–	Overtone of δ(CH) out of plane
1930 m		1739 vw		
1828 m				
1730 m				
1624 m	1645 m, 1629 m, 1450 m	1639 ms	–	$\delta(H_2O)$
1543 s	1421 m	1529 vs		ν(C=C); Py ring
1483 s		1461 vw		ν(C=N); Py ring
1454 m		1426 ms		
1414 m				
1388 m	1384 m, 1360 m, 1325 m	1387 ms	–	$\delta_{as}(CH_3)$
1329 m		1358 vw,sh		$\delta_s(CH_3)$
1279 vs	1295 m	1303 s	–	δ(C–O); –OH aliphatic
1215 vs	1234 m	1228 ms		ν(C–O); –OH phenolic
1088 s	1089 vw	1172 vw		
		1093 mw		
1018 vs	1053 vw, 990 vw	1027 vs	–	δ(C–C) in plane bend
991 vw				
–	–	955 s	–	ν(V=O)
965 m	752 w, 725 w, 692 vs	841 w	–	CH-deformation
925 w	533 m, 518 m, 477 m	781 m		
872 s	403 m, 357 m, 330 m	711 m		
801 s	288 m, 268 m	620 s		
748 s				
684 m				
–		577 vw		ν(V–O)
		548 vw		
		468 ms		

v very, *s* strong, *w* weak, *m* medium, *br* broad, *sh* shoulder

[a] ν stretching, *δ* bending

3 Results and discussion

3.1 Characteristic of the vanadyl$(VO)^{2+}$/vitamin B6 complex

Without X-ray single crystal analysis, no definite formula structures can be suggested. However, spectroscopic (infrared, UV–vis. and ESR), effective magnetic moment and elemental analyses data led us to predict structures. The colors, yield (%), conductivity, elemental analysis data and composition of the vanadyl$(VO)^{2+}$/vit B6 complex is given in Table 1. Accordingly, the VO^{2+}/vit B6 complex is agreement with square pyramidal geometry structure for similar complexes in literature [37–39]. The vanadyl$(VO)^{2+}$/vit B6 complex was synthesized with contain two equal moles of pyridoxine (vit B6) moiety. Based on the stoichiometry between vanadyl(VO) ion and pyridoxine ligand, the physical and analytical data (Table 1) for the synthesized vanadyl$(VO)^{2+}$/vit B6 complex is in good agreement with the proposed molecular formula viz. VO(vit B6)2·2H_2O.

3.1.1 Molar conductance

The molar conductance value of the VO^{2+}/vit B_6 complex (1.0×10^{-3} mol/cm^3) was determined in DMSO. This value was found at 23 ohm^{-1} cm^2 mol^{-1} indicating a non electrolytic nature [40]. The decreasing in the electrolytic nature of this complex is due to the absence of sulfate (SO_4^{2-}) ions within the coordination sphere. The absence of

Table 3 Magnetic moments and electronic spectral bands (nm) of the vit B_6 ligand and its VO^{2+} complex

Compounds	Magnetic moments μ_{eff}	Intraligand and charge transfer (nm)			Proposed geometry
		$\pi \rightarrow \pi^*$ transitions	$n \rightarrow \pi^*$ transitions	LMCT	
Vit B6	–	272, 288, 300, 314	375, 387	–	–
$[VO(vit\ B_6)_2]\cdot 2H_2O$	1.63	276, 316	356	408	Square pyramidal

Table 4 Electronic spectra, cm^{-1} of $[VO^{2+}(vit\ B_6)_2]\cdot 2H_2O$ complex

Compound	2B2 → 2E	2B2 → 2B1	2B2 → 2A1
$[VO(vit\ B6)2]\cdot 2H_2O$	14,225	16,447	22,222

sulfate ions in vanadyl$(VO)^{2+}$/vit B_6 complex was checked by the addition of saturated solution of barium chloride reagent.

3.1.2 Infrared and Raman spectra

Vibrational assignments for the diagnostic infrared spectral bands are discussed in Table 2 and referred below. Assignments have been given in comparison with the data obtained for free vit B_6 and vanadyl$(VO)^{2+}$/vit B_6 complex (assumed to contain a 'free' hydroxyl groups), by taking into account the structure of the complex and by studying literature reports for pyridoxine (vit B_6) complexes [37–39]. The ring stretching vibrations (C–C) are very much prominent in the spectrum of pyridine moiety for vitamin B_6 and its derivatives and are highly characteristic of the aromatic ring itself [41]. The five bands observed at 1624, 1543, 1483, 1454 and 1414 cm^{-1} are assigned to C–C stretching vibrations. The Raman counterpart of C–C stretching vibrational modes is identified at 1645, 1629, 1450 and 1421 cm^{-1}. The presence of nitrogen in the ring of the pyridine moiety gives rise two C–N stretching vibrations. Identifying these vibrations is rather a difficult task as their vibrational frequency lies within the C–C stretching region [40]. In the present work the bands at 1,483 and 1,279 cm^{-1} in pyridoxine free ligand are assigned to C–N stretching vibrations. In the FT Raman spectrum of free vit B_6 the C–N stretching vibrations are identified at 1,450 and 1,218 cm^{-1}. The bands observed at 1,018 and 991 cm^{-1} are assigned to the in-plane carbon bending vibrations. The carbon out-of-plane bending vibrations are observed at 684, 622, 596, 519 and 473 cm^{-1}. The hetro-aromatic structure of vit B_6 shows the presence of C–H stretching vibrations in the region 3,000–3,100 cm^{-1} [42] at 3,093 cm^{-1}, which is the characteristic region for ready identification of this structure. The bands exhibited at 965, 925, 872, 801 and 748 cm^{-1} are assigned to C–H out-of-plane deformations modes of aromatic ring. The four medium-to-very weak bands presence in the free vit B_6 ligand at 1996, 1930, 1828 and 1730 cm^{-1} are assigned to the overtone of δ(CH) out-of plane. In case of free vitamin B_6 ligand, the stretching vibrations of hydroxyl groups for both alcoholic and phenolic types are detected at 3,326 and 3,241 cm^{-1}. Also, the bending and stretching (ν(C–O)) vibrations spectra of –OH phenolic and alcoholic groups occurs at 1,215 and 1,088 cm^{-1}, respectively. The infrared spectrum of vit B6 gives a very strong band at 2,822 cm^{-1} and two medium bands at (1,388 and 1,329 cm^{-1}) attributed to stretching and bending vibration motions of $–CH_3$ methyl and $–CH_2$ methylene groups. According to the comparison between the full assignments of vitamin B6 free ligand mentioned above with the vanadyl$(VO)^{2+}$ complex, we can concluded that, the stretching and bending vibrations bands of hydroxyl for both phenolic and aliphatic are shifted or disappeared (Table 2), this due to the involvement of –OH phenolic group in position of (C3) and –OH of alcoholic group in position (C4) in the coordination behavior towards to vanadyl(VO) ion. The infrared absorption band of $VO(VO)^{2+}$ complex shows strong absorptions band at 955 cm^{-1} due to ν(V = O) due the presence of a double band in the VO^{2+} moiety. The interpretation of infrared spectra was supported that vitamin B6 acts as a bidentate ligand in anionic structure. Of the things striking the emergence of the Raman spectrum of vanadyl$(VO)^{2+}$ complex as a very strong broadening band without any detectable peaks, this, can be attributed to the fluorescence behavior of complex.

3.1.3 Electronic spectra and magnetic measurements

Tables 3 and 4 refer to the electronic (UV–vis and solid reflectance) spectra and magnetic measurements assignments which are important and interesting items for most chemical characterizations to draw important information about the structural aspects of the complexes. Pyridoxine HCl (vitamin B6) ligand, which is vital organic compound, has absorption in the ultraviolet region in the region of the 200–400 nm and in some cases these bands extends over to higher wavelength region due to conjugation. But upon complexation with vanadyl(VO) ion, due to interaction with the metal ion there will be an interesting change in the electronic properties of the system. New bands in the

visible region due to d–d absorption and charge transfer spectra from metal to ligand (M–L) or ligand to metal (L–M) can be observed and this data can be processed to obtain information regarding the structure and geometry of the complexes [43]. Electronic spectra (UV–visible) of free vit B6 ligand and vanadyl$(VO)^{2+}$ complex were recorded in DMSO with 10^{-3} mol/cm^3 corresponding to the $\pi \rightarrow \pi^*$ and $n \rightarrow \pi^*$ transitions. The first range can be assigned to $\pi \rightarrow \pi^*$ transitions in the aromaticity of pyridine ring while the second range is most probably due to the $n \rightarrow \pi^*$ transitions of OH groups beside to nitrogen atom of pyridine ring [44]. The third type of transition in visible region located at 408 nm for vanadyl$(VO)^{2+}$ complex can be attributed to the ligand-to-metal charge transfer bands LMCT from the electronic lone pairs of oxygen of hydroxyl group to the metal ions.

The magnetic moment for VO/vit B6 complex found to be 1.63 B.M. at room temperature, which is within the range of spin only value for one unpaired electron [45]. The diffuse reflectance spectrum of VO complex displays three bands at 14225, 16447 and 22222 cm^{-1} which may be assigned to the $^2B_2 \rightarrow 2E$, $^2B_2 \rightarrow {}^2B_1$ and $^2B_2 \rightarrow {}^2A_1$ transitions, respectively for square pyramidal geometry around VO ion.

3.1.4 *Electron spin resonance*

ESR spectroscopy is a useful technique as it provides information on the stereochemistry, ligand type and degree of covalence of oxovanadium (IV) complexes. The unpaired electron responsible for ESR spectrum is confined largely to the oxovanadium (IV) centre. Due to the strong vanadium–oxygen interaction in the oxovanadium unit, axial or nearly axial ESR spectra are usually observed for oxovanadium (IV) complexes. The ESR experimental and simulated spectra are reported in Fig. 1. The $g_{\|}(1.627) < g_{\perp}$ (1.825) relations is consistent with square pyramidal complexes with C_{4V} symmetry with the unpaired electron in the d_{xy} orbital [46].

3.1.5 *Scanning electron microscopy and X-ray powder diffraction*

The microstructure, surface morphology and chemical composition of pyridoxine HCl (vit B6) as a free ligand and vanadyl$(VO)^{2+}$ complex were studied using scanning electron microscopy. Typical scanning electron micrographs are shown in Fig. 2a, b. The surface morphology of SEM micrograph reveals the well sintered nature of the complexes with variant grain sizes and shapes. The distribution of the grain size of vanadyl$(VO)^{2+}$/vit B6 complex is homogeneous (rectangle shapes) although the free vit B6 ligand, Fig. 2a, has small-to-medium particles with different size. Clear large grains are obtained with agglomerates for vit B6 free ligand. The particle size distribution of the vanadyl$(VO)^{2+}$ complex was evaluated and the average particle size found to be 0.33 μm. Of the important results of the research is the conversion of agglomerate particles of free vit B6 to size 300 nm small particles upon the complexation with vanadyl ion.

The X-ray powder diffraction patterns in the range of $4° < 2\theta < 80°$ for the free vit B6 ligand and its vanadyl$(VO)^{2+}$ complex were carried in order to obtain an idea about the lattice dynamics of the resulted complex. The values of 2θ, d value (the volume average of the crystal dimension normal to diffracting plane), full width at half maximum (FWHM) of prominent intensity peak, relative intensity (%) and particle size of compounds were compiled in Table 5. The maximum diffraction patterns of vit B6 and vanadyl$(VO)^{2+}$ complex exhibited at 2θ/d-value(Å) = 20.73/4.281 and 6.874/12.850, respectively. The crystallite size could be estimated from XRD patterns by applying FWHM of the characteristic peaks using Deby-Scherrer Eq. 1 [47]

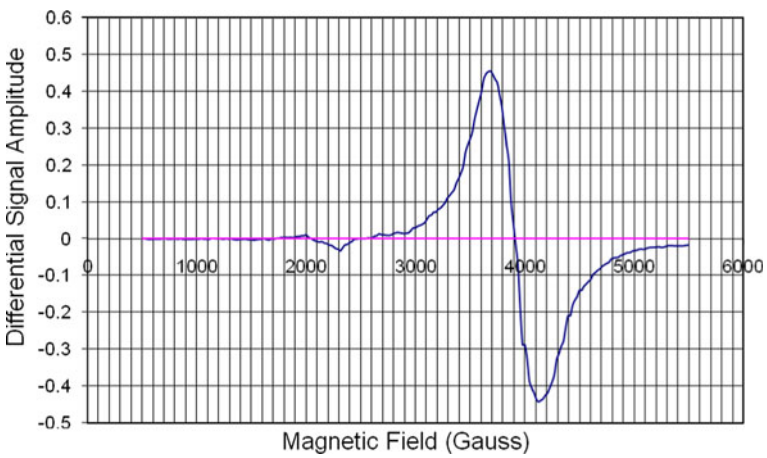

Fig. 1 ESR spectrum of [VO(vit B6)2]·2H_2O complex

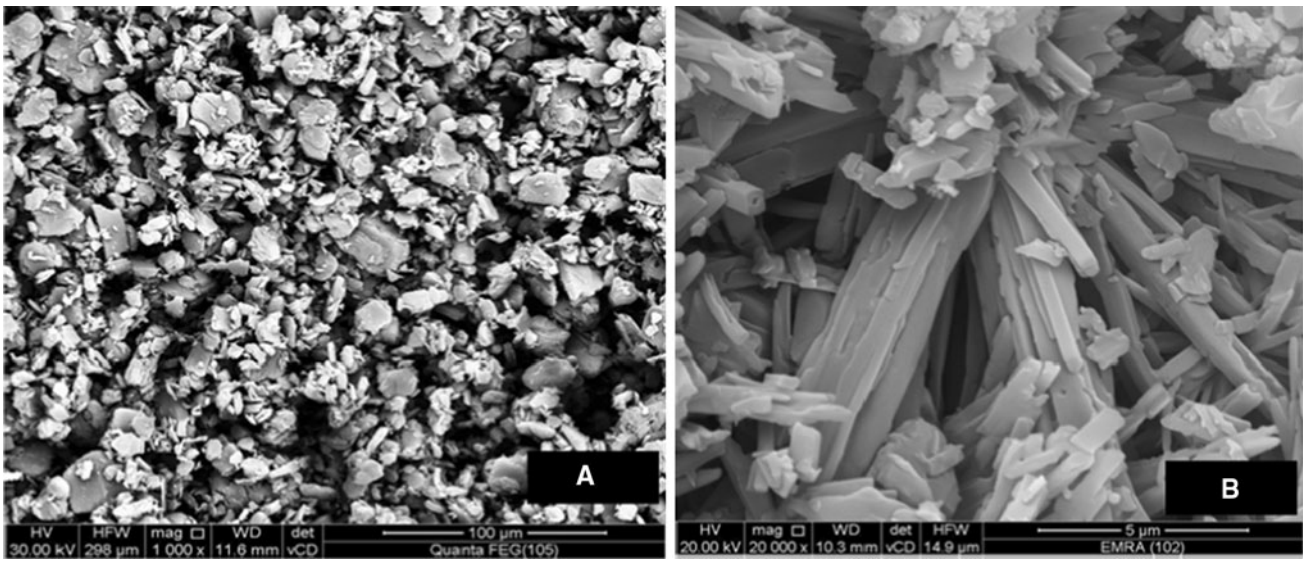

Fig. 2 SEM morphology of **a** vit B6·HCl and **b** $[VO(vitB6)2]\cdot 2H_2O$ complex

Table 5 XRD spectral data of the highest value of intensity of the vit B_6 ligand and its VO^{2+} complex

Compounds	2θ	d value	FWHM	Relative intensity (%)	Particle size (nm)
Vit B_6	20.730	4.281	0.001	100	155
$[VO(vit\ B_6)_2]\cdot 2H_2O$	6.874	12.849	0.001	100	146

$$D = K\lambda/\beta\cos\theta \quad (1)$$

where D is the particle size of the crystal gain, K is a constant (0.94 for Cu grid), λ is the X-ray wavelength (1.5406 Å), θ is the Bragg diffraction angle and β is the integral peak width. The particle size was estimated according to the highest value of intensity compared with the other peaks. These data gave an impression that the particle size of vanadyl$(VO)^{2+}$ complex located within nano scale range.

3.1.6 Thermal and kinetic estimations

The differential thermo gravimetric (DTG) gives information about thermal stability, melting, crystallization, decomposition, de-solvation, sublimation, and phase transformation. Any reaction or transformation involving absorption or release of heat can also be detected with this technique. The thermal and kinetic characteristic data of the complexes were determined from DTG thermo grams (melting points, taken as the temperature corresponding to the minimum of the endothermic peak) and the results are summarized in Fig. 3a, b. The DTG analyses were carried out mainly to determine the melting and the decomposition temperatures of the oxovanadium (IV) complexes because their melting points were outside the range covered by the melting point instrument. The DTG curve of free pyridoxine HCl ligand (Fig. 3a) shows a sharp endothermic peak with a maximum at 256 °C corresponding to the decomposition process. The ligand is stable up to 200 °C where decomposition starts and is completed at 800 °C. The thermal decomposition patterns of free vit B6. HCl can be suggested as follows;

$$C_8H_{11}NO_3\cdot HCl\ (\text{pyridoxine HCl}) \rightarrow HCl + NH_3 + 3C_2H_2 + CO_2 + H_2O + \downarrow C\ (\text{residual})$$

The TG curve of the VO complex shows three-step decomposition. The first step from 50 to 100 °C with a mass loss of 8.244 % (calcd. 8.195 %), accompanied by two endothermic peaks with tmax = 243 and 462 °C on the DTG curve, may be attributed to the decomposition of the two non-coordinated water molecules and two moieties of the ligand. The second and third steps, from 238 to 249 and 305 to 473 °C with a mass loss of 68.03 % corresponds to the removal of the gaseous molecules due to the decomposition of bi-functional vit B6 moieties. The end product, as the residue obtained is close to that expected for metal oxide VO2.5 polluted with only one carbon atoms. The suggested decomposition equation of the vanadyl$(VO)^{2+}$/vit B6 complexes can be speculated as follows;

$$VO(C_8H_{11}NO_3)_2\cdot 2H_2O \rightarrow VO(C_8H_{11}NO_3)_2 + 2H_2O \quad (i)$$

$$VO(C_8H_{11}NO_3)_2 \rightarrow 2NH_3 + 6C_2H_2 + 3^1/_2CO + H_2O + (VO_{2.5} + \downarrow C)\ \text{residual} \quad (ii)$$

The kinetic and thermodynamic parameters viz. the order of the reaction (*n*), the energy of activation (*E*a), the

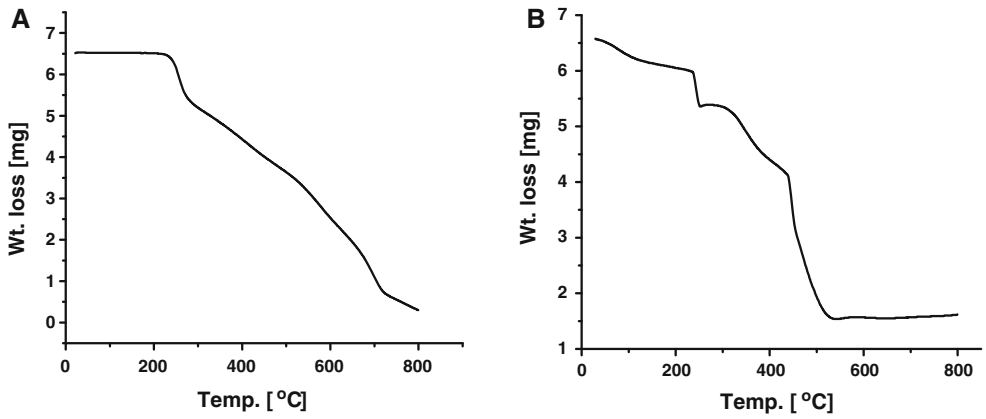

Fig. 3 TGA curves of **a** vit B6·HCl and **b** [VO(vitB6)2]·$2H_2O$ complex

Table 6 Kinetic parameters using the Coats–Redfern (CR) and Horowitz–Metzger (HM) equations for the vit B_6 ligand and its VO^{2+} complex

Compounds	Method	Parameter					r
		E (J mol^{-1})	A (s^{-1})	ΔS ($Jmol^{-1}K^{-1}$)	ΔH (J mol^{-1})	ΔG (J $mol^{-1)}$	
Vit B_6	CR	1.59×10^5	3.01×10^{13}	8.34	1.55×10^5	1.50×10^5	0.982
	HM	1.71×10^5	1.29×10^{15}	39.6	1.66×10^5	1.45×10^5	0.971
[VO(vit $B_6)_2$]·$2H_2O$	CR	1.51×10^6	1.75×10^{15}	2.67×10^3	1.50×10^6	1.29×10^5	0.964
	HM	1.54×10^6	3.07×10^{15}	2.73×10^3	1.54×10^6	1.32×10^5	0.965

pre-exponential factor (Z), the entropy of activation ($\Delta S\#$) and the Gibbs energy change ($\Delta G\#$), together with the correlation coefficient (r) for the non-isothermal decomposition of the VO complex, was determined by the Horowitz–Metzer (HM) approximation method [48] and the Coats–Redfern integral method [49]. The obtained data are given in Table 6. The results showed that the values obtained by two methods are comparable. The calculated values of the activation energy of the complexes are relatively high, indicating the thermal stability effect of the metal ion on the thermal decomposition of the complex [50, 51]. A positive change in entropy of activation indicates that the system has become more disordered. Degrees of freedom are "liberated" on going from the ground state to the transition state. The reaction is fast decomposed at the earlier temperatures.

3.1.7 Suggested structures

The newly synthesized vanadyl$(VO)^{2+}$/vit B6 complex was characterized using elemental analyses and different spectroscopic methods. On the basis of spectral data, 1:2 stoichiometries were found for the metal: ligand, the non-electrolytic nature of the studied complex showing the absence of sulfate anion. The magnetic and electronic spectral studies support a square pyramidal geometry for this complex. Based on the spectral data the proposed geometries of the studied complex are depicted in Fig. 4. The results of in vitro biocide activities of the ligand and its metal complexes clearly show that the compounds have both antibacterial and antifungal potency against the tested organisms. The complex showed more activity than free ligand.

3.2 Effect of new complex on the biochemical of diabetic mice

3.2.1 Body weight and blood glucose l

Normal healthy control was found to be stable in their body weight (Table 7). Body weight in the diabetic group was significantly lower when compared with the other groups. The final body weight in the diabetic group was significantly lower when compared with the as control group. Treatment the diabetic animals with vanadyl(II)/vit B6 compound did not improve the weight as compared to initial weight of mice after 30 days of treatment.

Figure 5 shows the initial and final sugar level for all treatment groups. Administration of alloxan (150 mg/kg) led to elevation of blood glucose levels to 210.29 ± 5.1–231.71 ± 69, which was maintained over a period of 4 weeks. The level of glucose was more decreased in

normal mice that treated with vanadyl$(VO)^{2+}$/vit B6 complex than in control negative group. Treatment of vanadyl$(VO)^{2+}$/vit B6 complex (40 mg/kg, i.p.) to diabetic group for 4 weeks led to fall decreased in glucose level.

Free radicals and oxidative stress may act as a common pathway to diabetes itself, as well as to its complications [52]. The characteristic loss of body weight associated with alloxan induced diabetes could be due to increased muscle wasting in diabetes [53]. The decrease in body weight observed in uncontrolled diabetics might be the result of excessive breakdown of tissue protein due to the unavailability of carbohydrate for utilization as an energy source [54]. When vanadyl sulfate (100 mg/kg) was administered to diabetic rat, the weight increased by 1.15 fold [55]. However, it could not normalize the body weight completely as it remained significantly lesser than normal controls. The present investigation showed that administration of vanadyl$(VO)^{2+}$/vit B6 complex compound improved the body weight in diabetic mice by 1.1 fold as compared to diabetic mice, which could be attributed to its antidiabetic and antihyperlipidemic role.

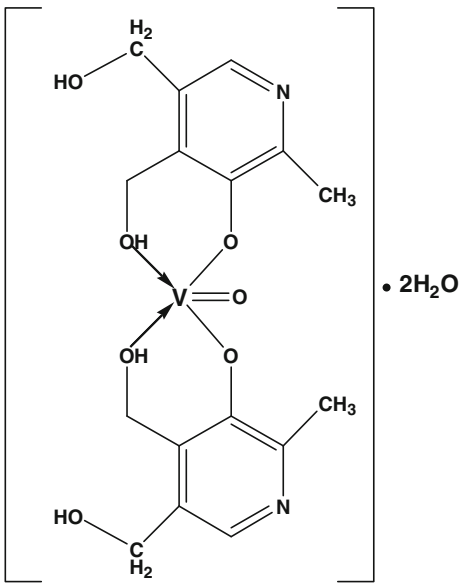

Fig. 4 Suggested structure of $[VO(vitB6)2]\cdot 2H_2O$ complex

The level of blood glucose increased in alloxan-induced mice by 45.34 % as compared to control as observed before by Mahesar et al. [56]. In the present study, treatment the diabetic mice with vanadyl$(VO)^{2+}$/vit B6 complex (40 mg/kg) each alternative day for 30 day decreased the blood glucose levels by 55.67 % as compared to diabetic mice. The present result is in accordance with other previous studies [57, 58]. Intraperitoneally injection of vanadyl sulfate and vanadate, reduce blood glucose levels in alloxan diabetic mice and STZ-diabetic rats to normal values [55, 59, 60]. Niu et al. [61] reported that vanadyl sulfate (0.06 mmol/kg) each alternative day for 30 day decreased the blood glucose levels by 13.09 % as compared to diabetic rat. Yanardag et al. [58] reported that oxovanadium (0.2 mM/kg) each alternative day for 12 day decreased the blood glucose levels by 62.85 % as compared to diabetic rat. There is small variance in the effect of vanadyl sulfate alone as in the previous studies and its combination with vit B6 as in the present study that could be related to the difference in the species, dose and the duration of the treatment. Numerous studies on vanadium compound suggest that these effects may be attributed to the insulin mimetic effect of vanadyl sulfate in various tissues [55, 59]. In vivo study, vanadyl sulfate increases glucose transport and metabolism in skeletal muscle, liver and adipose tissue [60].

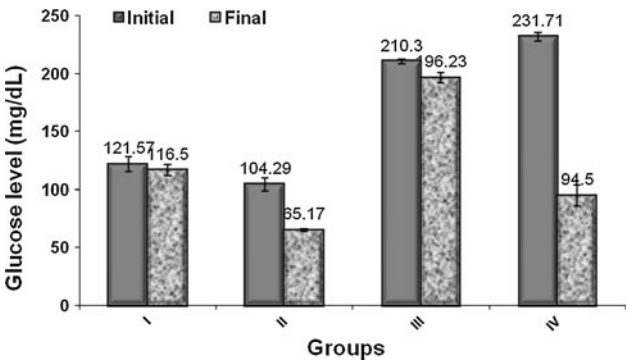

Fig. 5 Effect of VO^{2+}/vit B6 complex on the blood glucose levels in normal and diabetic mice. *I* control, *II* vanadyl$(VO)^{2+}$/vit B6 complex (40 mg/kg, i.p), *III* diabetic induced with alloxan (150 mg/kg), *IV* diabetic treated with vanadyl$(VO)^{2+}$/vit B6 complex (40 mg/kg, i.p)

Table 7 Effect of vanadyl$(VO)^{2+}$/vit B_6 complex on the body weight in normal and diabetic mice

Weight/groups	I	II	III	IV
Initial (g)	26.62 ± 0.57	28.33 ± 0.88	30.02 ± 0.11	29.58 ± 0.37
Final (g)	23.33 ± 0.8[a]	27.33 ± 0.56	32.27 ± 0.41	26.33 ± 0.56

Data presented as mean ± S.E. (n = 8–10)

I control, *II* vanadyl$(VO)^{2+}$/vit B_6 complex (40 mg/kg, i.p), *III* diabetic induced with alloxan (150 mg/kg), *IV* diabetic treated with vanadyl$(VO)^{2+}$/vit B_6 complex (40 mg/kg, i.p)

[a] Significant different as compared to the initial value

3.2.2 Glucose tolerance test (GTT)

Glucose (2 g/kg body weight) was given intraperitoneally and blood glucose level was measured at 0, 30, 60, 90, and 120 min (Fig. 6). The glucose tolerance curve in the vanadyl$(VO)^{2+}$/vit B6 complex treated-normal group was lower than that in the control group, suggesting that vanadyl$(VO)^{2+}$/vit B6 complex decrease influence the glucose tolerance in normal mice. In the diabetic group, the blood glucose levels showed a typical diabetic response to a glucose loading. However, vanadyl$(VO)^{2+}$/vit B6 complex administration for 30 day to diabetic mice was markedly lowered the blood glucose levels in GTT. It showed that the complex could accelerate the glucose clearance and improve glucose tolerance in alloxan diabetic mice.

3.2.3 Complete blood picture (CBP)

Table 8 represents effect of vanadyl$(VO)^{2+}$/vit B6 complex on the hematological parameters in normal and diabetic mice during the 30 days exposure. The level of RBCs, Hb, HCT, MCH and WBCs decreases in diabetic mice as compared to the control group. The level of RBCs, Hb, HCT, MCH and WBCs decreased in diabetic treated mice with vanadyl$(VO)^{2+}$/vit B6 complex as compared to the diabetic mice by 13.1, 37.8, 36.9 and 21.8 %. The platelets level was increase compared to the control group. However, there were decreases significant in the number of platelets and WBCs in vanadyl$(VO)^{2+}$/vit B6 complex compared to the diabetic group by 11.9 and 35.2 %, respectively.

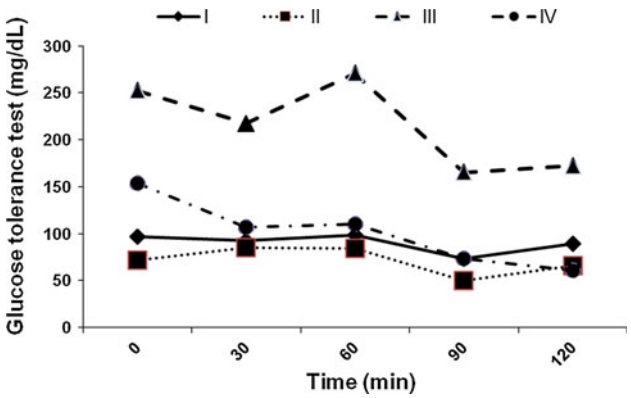

Fig. 6 Effect of VO^{2+}/vit B6 complex on the glucose tolerance test in normal and diabetic mice. *I* control, *II* vanadyl$(VO)^{2+}$/vit B6 complex (40 mg/kg, i.p), *III* diabetic induced with alloxan (150 mg/kg), *IV* diabetic treated with vanadyl$(VO)^{2+}$/vit B6 complex (40 mg/kg, i.p)

The excess of glucose is present in the blood during diabetes, which react with hemoglobin and form glycosylated hemoglobin. The various proteins including hemoglobin, crystalline proteins undergo nonenzymatic glycation in diabetes [62]. Reduction in RBCs and Hb were observed in diabetic mice (Table 8). Reactive oxygen species have been implicated in the mechanism of damage of red blood cells in diabetic patients [63]. As a result, hematological complications develop which consist mainly of abnormalities in the function, morphology and metabolism of erythrocytes, leukocytes and platelets [64]. It has been suggested that anemia occurrence in DM is due to the increased non-enzymatic glycosylation of RBC membrane proteins, which correlates with hyperglycemia [65]. Oxidation of these glycosylated membrane proteins and hyperglycemia in DM cause an increase in the production of lipid peroxides causing a haemolysis of RBC through many pathological consequences [66]. The major pathological consequences of free radical induced membrane lipid peroxidation include increased membrane rigidity, decreased cellular deformability, reduced erythrocyte survival, and lipid fluidity [67]. Treatment the diabetic mice with vanadyl$(VO)^{2+}$/vit B6 complex increased in RBCs and Hb by $\sim$13.07 and $\sim$37.82 %, respectively as compared to diabetic mice.

In the present study, platelet aggregation was significantly higher in diabetic group compared with control group these results were in agreement with Vericel et al. [68]. The first mechanism explaining increased platelet

Table 8 Effect of vanadyl$(VO)^{2+}$/vit B6 complex on the hematological parameters in normal and diabetic mice

Groups	RBCs (10^6/mm3)	Hb (g/dl)	HCT (%)	MCH (pg)	MCV (fl)	MCHC (g/dl)	Platelets (10^3/mm^3)	WBCs (10^3/mm^3)
I	8.91 ± 0.22	13.93 ± 0.29	47.63 ± 0.30	15.30 ± 0.15	52.57 ± 0.88	29.07 ± 0.78	534.67 ± 27.09	8.63 ± 0.14
II	8.98 ± 0.31	13.37 ± 0.63	39.07 ± 1.17	13.67 ± 0.09	44.10 ± 0.38	31.03 ± 0.20	570.00 ± 15.28	1.30 ± 0.15
III	7.57 ± 0.20	10.47 ± 0.20[a]	34.53 ± 1.53[a]	13.77 ± 0.09	45.27 ± 0.82[a]	30.40 ± 0.78	662.67 ± 35.18	5.71 ± 0.84
IV	8.56 ± 0.21	14.43 ± 0.29[b]	47.30 ± 1.56[b]	16.77 ± 0.09	54.73 ± 0.41[b]	30.40 ± 0.40	583.33 ± 7.51	3.70 ± 0.81

Data presented as mean ± S.E. ($n = 5$). All the data measured by cell counter (Sysmex, model KX21N)

I control, *II* vanadyl$(VO)^{2+}$/vit B_6 complex (40 mg/kg, i.p), *III* diabetic induced with alloxan (150 mg/kg), *IV* diabetic treated with vanadyl$(VO)^{2+}$/vit B_6 complex (40 mg/kg, i.p)

[a] Significant different as compared to control animals

[b] Significant different as compared to diabetic animals

reactivity is increased mean platelet volume. The second mechanism explaining increased platelet reactivity could be due to reduced production of factors that inhibit platelet activation, in particular NO [69]. In platelets from diabetic patients, platelet NO· synthases (NOS) activity is significantly lower than that measured in platelets from healthy subjects which leads to reduced platelet activation, suggesting that the decreased NOS activity might play a role in the pathogenesis of diabetic vascular complications [70]. Excessive production of reactive oxygen species (ROS) represents the third mechanism explaining increased platelet reactivity in DM [71]. Treatment the diabetic mice with vanadyl$(VO)^{2+}$/vit B6 complex decreased in platelets by 11.97 % as compared to diabetic mice (Table 8). Oral injection vitamin E (7 mg/kg) or vitamins E and C (7 mg/kg) each alternative day for 30 day decreased the platelets by 5.81 and 9.30 %, respectively as compared to diabetic rat [72].

The significant increase in WBCs count in diabetic mice when compared to the control group may be due to alloxan poisoning [73]. This is line with normal physiological response following the perception of an assault by the body defense mechanisms [27]. Treatment the diabetic mice with vanadyl $(VO)^{2+}$/vit B6 complex decreased in WBCs by 35.20 % as compared to diabetic mice (Table 8).

3.2.4 Lipid profile

Table 9 shows that the administration of alloxan (150 mg kg^{-1} bw) increases the total cholesterol (TC), triglycerides (TG), LDL-c and VLDL-c levels; these increase in TC, TG, LDL-c and VLDL-c were ~3.3-, 1.3-, 5.9- and 1.3-fold ($P \leq 0.001$), respectively, after 30 days, as compared to control mice. The administration of vanadyl $(VO)^{2+}$/vit B6 complex countered the increase in TC, TG, LDL-c and VLDL-c (Table 10) levels at the end of treatment. Reduction of serum HDL-c levels in diabetic mice was observed. This result was more evident 79.74 % ($P \leq 0.01$) after 30 days of treatment. In diabetic animals, the treatment with vanadyl$(VO)^{2+}$/vit B6 complex decreased the serum LDL-c levels by 79.13 %. The present study showed that the vanadyl$(VO)^{2+}$/vit B6 complex led to significant improvement in the lipid metabolism parameters in the serum of diabetic mice. Risk ratio and atherogenic index in blood serum were significantly increased in diabetic mice ($P \leq 0.01$). Administration vanadyl$(VO)^{2+}$/vit B6 complex reversed these effects (Table 9).

In the present study, there were significantly increased in the levels of serum TC, TG and LDL-c but markedly decreased level of serum HDL-c in alloxan induced diabetic mice as reported before by Bolkent et al. [59, 74, 75]. The abnormal high levels of serum lipids in the diabetic animals is mainly due to the increased the mobilization of free fatty acids from the peripheral deposits, since insulin inhibits the hormone sensitive lipase [76]. Excess fatty acids in the serum of diabetic mice are converted into phospholipids and cholesterol in the liver. Liver, an insulin

Table 10 Effect of vanadyl$(VO)^{2+}$/vit B_6 complex on the activities of lactate dehydrogenase (LDH) and glucose-6-phosphate dehydrogenase (G6PD) in normal and diabetic mice

Groups	LDH (U/L)	G6PD (U/L)
I	287.28 ± 25.44	12.83 ± 0.69
II	65.52 ± 10.84a	11.72 ± 0.36
III	425.88 ± 52.22a	8.81 ± 0.32a
IV	272.16 ± 48.24b	11.32 ± 0.40b

Data presented as mean ± S.E. (n = 8–10)

I control, *II* vanadyl$(VO)^{2+}$/vit B_6 complex (40 mg/kg, i.p), *III* diabetic induced with alloxan (150 mg/kg), *IV* diabetic treated with vanadyl$(VO)^{2+}$/vit B_6 complex (40 mg/kg, i.p)

[a] Significant different as compared to control mice

[b] Significant different as compared to diabetic mice

Table 9 Effect of vanadyl$(VO)^{2+}$/vit B6 complex on the lipid profile in normal and diabetic mice

Groups	Cholesterol (mg/dl)	Triglyceride (mg/dl)	HDL-c (mg/dl)	LDL-c (mg/dl)	VLDL (mg/dl)	Risk ratio	Atherogenic index
I	78.42 ± 5.79	173.37 ± 8.85	36.83 ± 2.87	36.38 ± 4.60	34.6 7 ± 1.77	2.21 ± 0.33	1.21 ± 0.33
II	79.47 ± 6.57	98.91 ± 4.21a	46.29 ± 2.17a	49.52 ± 7.05	19.78 ± 0.84	1.58 ± 0.18	0.58 ± 0.56
III	262.11 ± 11.02a	226.01 ± 10.65a	7.46 ± 0.50a	215.40 ± 9.93a	45.22 ± 2.13	35.86 ± 3.56	34.86 ± 3.56
IV	76.63 ± 1.71b	142.61 ± 10.86b	15.85 ± 0.99b	44.94 ± 2.47b	28.52 ± 2.17	4.90 ± 0.26	3.90 ± 0.26

Data presented as mean ± S.E. (n = 7–8). Low density lipoprotein cholesterol (LDL-c) = Total cholesterol—(HDL-c + triglyceride)/5, volatile low density lipoprotein cholesterol (VLDL-c) = Triglycrid/5, Risk ratio = Total cholesterol/high density lipoprotein cholesterol (HDL- c), Atherogenic index = total cholesterol—(HDL-c/HDL-c)

I control, *II* vanadyl$(VO)^{2+}$/vit B_6 complex (40 mg/kg, i.p), *III* diabetic induced with alloxan (150 mg/kg), *IV* diabetic treated with vanadyl$(VO)^{2+}$/vit B_6 complex (40 mg/kg, i.p)

[a] Significant different as compared to control mice

[b] Significant different as compared to diabetic mice

dependent tissue that plays a pivotal role in glucose and lipid homeostasis and it is severely affected during diabetes [77]. Diabetes results in decrease in glucose utilization and an increase in glucose production in insulin-dependent tissues, such as liver [55]. The degree of hypercholesterolemia is directly proportional to severity in diabetes. In the present study, treatment the diabetic mice with vanadyl$(VO)^{2+}$/vit B6 complex (40 mg/kg, i.p) each alternative day for 30 day decreased the TC by 70.76 % as compared to diabetic mice. Administration of vanadyl sulfate only to alloxan diabetic mice normalizes serum levels of cholesterol. In current investigation, the TC, TG, LDL-c and VLDL decreased by 70.76, 36.90, 79.13 and 36.9, respectively after vanadyl$(VO)^{2+}$/vit B6 complex treatment of alloxanated mice. However, using vanadyl sulphate only decreased the TC, TG, LDL-c and VLDL by 25.31, 14.41, 57.43 and 20.49 %, respectively [55]. The underlying mechanism by which vanadyl sulfate exerts its cholesterol lowering effect seems to be a decrease in cholesterol absorption from the intestine, by binding with bile acids within the intestine and increasing bile acids excretion [78]. However, Sharma et al. [79] reported that vanadyl sulfate acts by decreasing the cholesterol biosynthesis especially by decreasing the 3-hydroxy-3-methylglutaryl-CoA (HMG-CoA) reductase activity, a key enzyme of cholesterol biosynthesis and/or by reducing the NADPH required for fatty acids and cholesterol biosynthesis. In addition, vanadyl may improve hypercholesterolemia by modifying lipoprotein metabolism: enhanced uptake of LDL by increasing LDL receptors [80], and/or by increasing the lecithin cholesterol acyl transferase activity [81], which may contribute to the regulation of blood lipids. HDL-c is recognized as a factor that protects against development of atherosclerotic disease, and low HDL-c is associated with an increased risk of coronary heart disease in individuals both with and without diabetes [82]. TC/HDL and LDL/HDL-c ratios are also predictor of coronary risk [55]. In the present study, mice treated with vanadyl$(VO)^{2+}$/vit B6 complex had markedly reduced these ratios. These results indicated that vanadyl$(VO)^{2+}$/vit B6 complex might have some protective effects against hypercholesterolemia risks in diabetes. In present study, diabetic mice exhibited abnormalities in lipid metabolism as evidenced from the significant elevation of VLDL-c level and atherogenic index. Treatment with vanadyl$(VO)^{2+}$/vit B6 complex for 30 days significantly and greatly reduced VLDL-c level and decreased of atherogenic index in diabetic mice indicating its potent antihyperlipidemic activity. Intraperitoneally administration of vanadyl vit B6 complex to alloxan diabetic mice reduced serum triglycerides levels by 36.9 %. These results are in agreement with the present finding that it is a very desirable biochemical state for prevention of atherosclerosis.

3.2.5 *Lactate dehydrogenase and glucose-6-phosphate dehydrogenase activities*

In alloxan diabetic mice the activity of serum LDH was significantly increased compared to control group (Table 10). The administration of vanadyl$(VO)^{2+}$/vit B6 complex to alloxan diabetic mice decreased the activities of LDH compared to diabetic group by 36.1 % ($P \leq 0.04$). In alloxan diabetic mice the activity of serum G6PD was significantly decreased ($P \leq 0.03$). The administration of vanadyl$(VO)^{2+}$/vit B6 complex to alloxan diabetic mice increased the activities of G6PD compared to diabetic group by 1.3-fold (Table 10).

The significant increases of LDH are mainly due to leakage of these enzymes into the blood because of alloxan toxicity in liver [83]. Treatment the diabetic mice with vanadyl$(VO)^{2+}$/vit B6 complex (40 mg/kg) each alternative day for 30 day decreased LDH by 36.1 % as compared to diabetic mice. Hussain [16] reported that the administration of vitamins E complex with vanadyl sulfate (100 mg/kg) each alternative day for 30 day decreased LDH by 19.69 % as compared to diabetic rat. This proved that vanadyl $(VO)^{2+}$/vit B6complex is improved the level of LDH in serum more than the vanadyl sulfate with vitamin E.

G6PD is the principal source of the major intracellular reductant, NADPH, which is required by many enzymes, including enzymes of the antioxidant pathway [84]. The level of G6PD decreased in alloxanated mice by 45.62 % as compared to control (Table 10), the same observations have been reported previously [85, 86]. Treatment the diabetic mice with vanadyl$(VO)^{2+}$/vit B6 complex increased G6PD by 28.49 % as compared to diabetic mice (Table 10). Hussain [16] reported that the administration of vitamins E complex with vanadyl sulfate (100 mg/kg) increased G6PD by 11.37 % as compared to diabetic rat. The present study declared that the vanadyl $(VO)^{2+}$/vit B6 complex enhanced the G6PD more than vanadyl sulfate with vitamins E by 2.5-fold. However, oral injection of pioglitazone (2.7 mg/kg) or metformin (180 mg/kg) each alternative day for 21 days significant increase in G6PD activity by $\sim$20 and $\sim$10.31 %, respectively as compared to diabetic rat [86].

3.2.6 *Uric acid and creatinine levels*

The results revealed a significant decrease in serum uric acid level ($P \leq 0.001$) in diabetic mice compared to control group (Table 11). Vanadyl$(VO)^{2+}$/vit B6 complex significantly increased ($P \leq 0.001$) uric acid level as compared to diabetic mice by 1.5-fold after 30 days of its administration. The results revealed a significant increased in serum creatinine level ($P \leq 0.002$) in diabetic groups compared to control group. Vanadyl$(VO)^{2+}$/vit B6

complex significantly decrease ($P \leq 0.03$) creatinine level compared to diabetic mice by 28.3 % after 30 days of its administration (Table 11).

The decrease in uric acid observed in diabetic mice is coinciding with the findings of Gawronska-Szklarz et al. [87] and Ashakiran et al. [88]. The previous investigation found that the uric acid decreased in diabetic mice and this decline may be due to the inhibited oxidative phosphorylation processes which lead to decrease of protein synthesis, increase in the catabolic processes and reduction of protein absorption [89]. Possible defects in tubular reabsorption and probably increased excretion may explain such decreases in blood uric acid [90]. In the present study, the administration of vanadyl$(VO)^{2+}$/vit B6 complex increased the uric acid by 45.63 % as compared to diabetic mice. There was no data available about the effect of vanadyl sulfate alone or its combination with any vitamin on the uric acid. There was other compounds cause increase in uric acid in diabetic rat [72, 91] but their effect less than vanadyl $(VO)^{2+}$/vit B6 complex. Oral injection of vitamin E or vitamin C (7 mg/kg) each alternative day for 30 day increased the uric acid by 4.38 % as compared to diabetic rat [72].

Measuring serum creatinine is a simple test most commonly used indicator of renal function, increasing of creatinine levels indicator of post stage of kidney failure. Creatinuria occurs in any condition associated with extensive muscle breakdown as in starvation and poorly controlled DM [90]. Creatinine concentrations strongly suggested impairment of kidney function in diabetes [91]. Results indicated that no-influence on the levels of creatinine in group with vanadyl$(VO)^{2+}$/vit B6 complex compared to control mice. This indicated that the vanadium complex has no side effect on kidneys tissue in animal model system under conditions of present experiments. Hussain [16] reported that the administration of vitamins E complex with vanadyl sulfate (100 mg/kg) each alternative day for 30 day to diabetic rat decreased the creatinine by 26.47 % as compared to diabetic rat. In the present study, treatment of the diabetic mice with vanadyl$(VO)^{2+}$/vit B6 complex (40 mg/kg) each alternative day for 30 day decreased the creatinine by 28.33 % as compared to diabetic mice (Table 11). Comparing the present study with previous investigation [16] indicated that vit B6/vanadyl compound enhanced the level of creatinine in serum more than vitamins E complex with vanadyl sulfate the serum compared.

Table 11 Effect of vanadyl$(VO)^{2+}$/vit B_6 complex on the uric acid and creatinine levels in normal and diabetic mice

Groups	Uric acid (mg/dl)	Creatinine (mg/dl)
I	4.93 ± 0.28	1.62 ± 0.12
II	3.49 ± 0.31[a]	1.45 ± 0.34
III	2.98 ± 0.14[a]	3.0 ± 0.23[a]
IV	4.34 ± 0.21[b]	2.15 ± 0.03[b]

Data presented as mean ± S.E. ($n = 8$–10)

I control, *II* vanadyl$(VO)^{2+}$/vit B_6 complex (40 mg/kg, i.p), *III* diabetic induced with alloxan (150 mg/kg), *IV* diabetic treated with vanadyl$(VO)^{2+}$/vit B_6 (40 mg/kg, i.p)

[a] Significant different as compared to control mice

[b] Significant different as compared to diabetic mice

3.2.7 *Oxidative and antioxidant*

3.2.7.1 Lipid peroxidation level LPO levels were found to be significantly increased in liver and kidney tissue for diabetic group than in the other groups ($P \leq 0.0001$) (Fig. 7). The LPO levels were significantly higher ($P \leq 0.0001$) in diabetic mice than in other groups by 2.7- and 9.3-fold for liver and kidney tissue, respectively. Vanadyl$(VO)^{2+}$/vit B6 complex given to the diabetic mice lowered the LPO levels in diabetic mice.

LPO is supposed to cause the destruction and damage of cell membranes leading to changes in membrane permeability and fluidity, enhancing the protein degradation in mice [92]. In the present study, the levels of LPO were increased indicating an increased in the generation of free radicals in the liver and kidney tissues of diabetic mice [93]. After administration of vanadyl$(VO)^{2+}$/vit B6 complex for 30 days to diabetic mice, the LPO were decreased in the liver and kidney tissues of diabetic mice (Fig. 7) indicating an decreased in the generation of free radicals. It has been reported that the vanadyl ion can act as a scavenger of oxyradicals and thus could prevent liver damage [57]. According to the present data, vanadyl $(VO)^{2+}$/vit B6 complex has a protective effect by decreasing LPO.

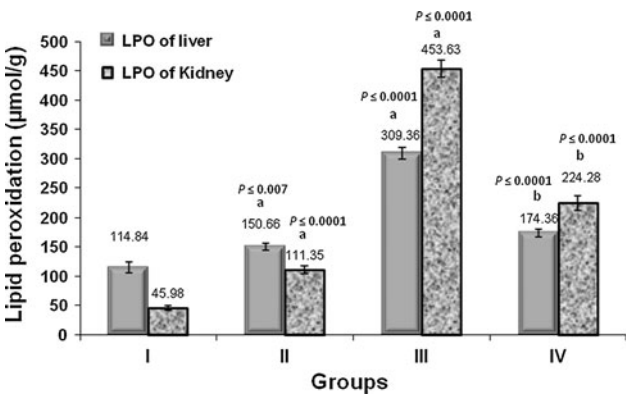

Fig. 7 Effect of VO^{2+}/vit B6 complex on the lipid peroxidation in normal and diabetic mice. *I* control, *II* vanadyl$(VO)^{2+}$/vit B_6 complex (40 mg/kg, i.p), *III* diabetic induced with alloxan (150 mg/kg), *IV* diabetic treated with vanadyl$(VO)^{2+}$/vit B_6 complex (40 mg/kg, i.p). [a] Significant different as compared to control mice. [b] Significant different as compared to diabetic mice

Table 12 Effect of vanadyl$(VO)^{2+}$/vit B_6 complex on superoxide dismutase (SOD), glutathione-S-transferase (GST) and total antioxidant capacity (TAC) in liver and kidney tissues of normal and diabetic mice

Parameters	Liver				Kidney			
	I	II	III	IV	I	II	III	IV
SOD (U/mg)	1.76 ± 0.22	1.64 ± 0.13[a]	0.89 ± 0.16[a]	1.53 ± 0.1 4[b]	1.04 ± 0.24	1.88 ± 0.25[a]	0.81 ± 0.17[a]	2.01 ± 0.33[b]
GST (U/mg)	97.48 ± 4.11	155.60 ± 3.59[a]	212.77 ± 21.45	77.24 ± 4.37[b]	79.99 ± 4.18	136.85 ± 14.15[a]	296.20 ± 21.75	106.48 ± 9.0[b]
TAC (%)	100.00 ± 1.00	96.75 ± 15.10	40.71 ± 8.90[a]	71.67 ± 17.90[b]	100.00 ± 1.00	114.79 ± 8.41	79.25 ± 4.77[a]	122.5 ± 9.44[b]

Data presented as mean ± S.E. (n = 8–10)

I control, *II* vanadyl$(VO)^{2+}$/vit B_6 complex (40 mg/kg, i.p), *III* diabetic induced with alloxan (150 mg/kg), *IV* diabetic treated with vanadyl $(VO)^{2+}$/vit B_6 complex (40 mg/kg, i.p)

[a] Significant different as compared to control mice

[b] Significant different as compared to diabetic mice

3.2.7.2 Superoxide dismutase and glutathione-S-transferase activities A significant decrease was observed in the activities of SOD in liver and kidney tissue of diabetic mice compared to control group by 49.3 and 22.1 %, respectively ($P \leq 0.01$) (Table 12). The SOD activities significantly increased ($P \leq 0.01$ and $P \leq 0.05$) in liver and kidney tissue of diabetic group treatment with vanadyl$(VO)^{2+}$/vit B6 complex when compared with diabetic group by 1.7- and 2.5-fold, respectively. In the mice exposed to alloxan of GST activity increased in liver and kidney tissue by 2.2- and 3.7-fold, respectively ($P \leq 0.001$) compared to control group respectively (Table 12). In diabetic mice treated with vanadyl$(VO)^{2+}$/vit B6 complex, the liver and kidney GST activity levels significantly decreased when compared with the diabetic group by 63.6 and 64 %, respectively.

Pourkhalili et al. [94] reported that SOD decrease in plasma and liver tissue of diabetic rat. SOD scavenged the superoxide radical by converting it into H_2O_2 and molecular oxygen. It is known that the SOD activity is low in DM [93]. The present study has results supporting this literature data. The reduced activity of SOD could be due to its depletion or inhibition as a result of the increased production of free radicals. The administration of vanadium (0.2 mM/kg) each alternative day for 12 day increased the activity of SOD in pancreas tissue and may help to control free radicals in diabetic rats by 9.32 % [58]. In the present study, the administration of vanadyl$(VO)^{2+}$/vit B6 complex increased the activity of SOD in liver and kidney tissues and may help to control free radicals in diabetic mice by 98 and 28 %, respectively.

GST plays a crucial role in the detoxifying mechanisms of drugs and xenobiotics by preventing the binding of reactive metabolites to cellular proteins, and modulating the by-products of oxidative stress by catalyzing the conjugation of electrophilic moieties to GSH [95]. GST distribution in the tissues may play an important role in the etiology, pathology and prevention of diabetes [96]. Moreover, Treatment the diabetic mice with vanadyl$(VO)^{2+}$/vit B6 complex decreased in GST activity in liver and kidney by 63.69 and 64.05 %, respectively as compared to diabetic mice (Table 12).

3.2.7.3 Glutathione level The liver and kidney GSH levels were significantly reduced in diabetic mice compared with the control group by 75 and 82 % ($P \leq 0.001$), respectively (Fig. 8). In diabetic mice treated with vanadyl(VO)/vit B6 complex, the liver and kidney GSH levels significantly increased ($P \leq 0.0001$) when compared with the diabetic group by 5.4- and 3.2-fold, respectively (Fig. 9).

Chronic hyperglycemia induced toxicity may also decrease the level of GSH in liver tissues [57, 93]. The

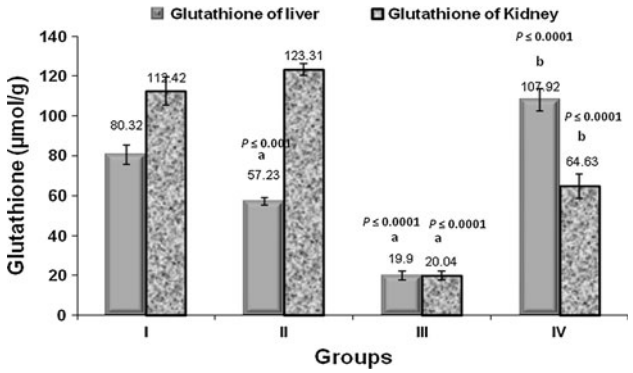

Fig. 8 Effect of VO^{2+}/vit B_6 complex on the glutathione in normal and diabetic mice. *I* control, *II* vanadyl$(VO)^{2+}$/vit B_6 complex (40 mg/kg, i.p), *III* diabetic induced with alloxan (150 mg/kg), *IV* diabetic treated with vanadyl$(VO)^{2+}$/vit B_6 complex (40 mg/kg, i.p).[a] Significant different as compared to control mice. [b] Significant different as compared to diabetic mice

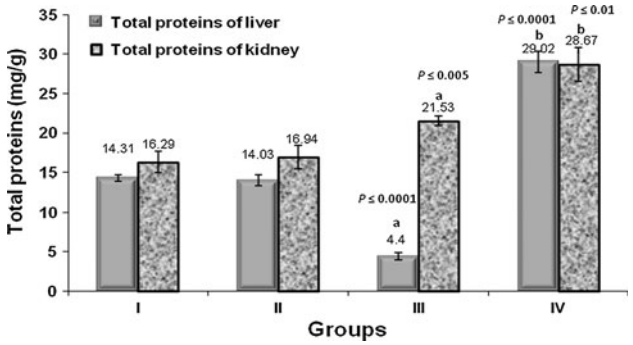

Fig. 9 Effect of VO^{2+}/vit B_6 complex on the total proteins in normal and diabetic mice. *I* control, *II* vanadyl$(VO)^{2+}$/vit B_6 complex (40 mg/kg, i.p), *III* diabetic induced with alloxan (150 mg/kg), *IV* diabetic treated with vanadyl$(VO)^{2+}$/vit B_6 complex (40 mg/kg, i.p). [a] Significant different as compared to control mice. [b] Significant different as compared to diabetic mice

levels of GSH in the liver and kidney tissues were decrease in diabetic mice (Fig. 8). These results are in agreement with those obtained by Rajasekaran et al. [93] and Koyuturk et al. [57]. This may be attributed to the unavailability of GSH. The possible mechanism for β-cell destruction by alloxan has been reported to include generation of some types of oxygen free radicals and alternation of endogenous scavengers of these reactive species. In the present study, hepatic and kidney GSH decreased significantly by 65.2 and 83.7 %, respectively in diabetic mice as compared to control group (Fig. 8). The intraperitoneally injection of vanadyl sulfate (100 mg/kg) each alternative day for 60 day increased the GSH in stomach tissue by 60.96 % [55] and in aorta by 89.3 % [60] in diabetic rat. Ravi et al. [54] reported that intraperitoneally injection of vanadium (0.2 mM/kg) each alternative day for 12 day increased the GSH in pancreas by 4.57 % in diabetic rat. These observations are in accordance with the findings that alloxan results in hepatic GSH content depletion in mice due to the higher level of free radical generation that convert more reduced GSH to its oxidized form [58]. In the present study, LPO and GSH turned toward its normal values. These results suggest that the administration of vanadyl$(VO)^{2+}$/vit B6 complex may have a protective effect against liver and kidney tissues damage in pro-oxidant conditions during diabetes.

3.2.7.4 Total antioxidant capacity content The liver and kidney total antioxidant capacity (TAC) levels were significantly reduced and reached to 40.7 and 79.3 % in the diabetic animals when compared to control group ($P \leq 0.05$ and $P \leq 0.04$), respectively (Table 12). In diabetic mice treated with vanadyl$(VO)^{2+}$/vit B6 complex, the liver and kidney FRAP levels significantly increased ($P \leq 0.04$ and $P \leq 0.005$) when compared with the diabetic group and reached to 71.7 and 122.5 %, respectively.

Oxidative stress in diabetes coexists with a reduction in the TAC, which can increase the deleterious effects of free radicals. Increased oxidative stress is believed to play an important role in the etiology and pathogenesis of chronic complications of diabetes [53]. A significant decreased level of TAC was observed in diabetic mice as compared to control group (Table 12). Glucose itself and hyperglycemia-related increased protein glycosylation are important sources of free radicals. Elevated glucose causes slow but significant non-enzymatic glycosylation of proteins in diabetes. In the administration of vanadyl$(VO)^{2+}$/vit B6 complex (40 mg/kg) increased the TAC in the liver and kidney by 43 and 35 % as compared to diabetic mice, respectively. Intraperitoneally injection of cerium oxide (60 mg/kg) each alternative day for 2 week increased the TAC in the plasma and liver by 3.22 and 19.31 %, respectively as compared to diabetic rat [94].

3.2.7.5 Total proteins content The liver total protein levels were significantly decreased in the diabetic mice when compared to control group by 69 % ($P \leq 0.0001$) (Fig. 9). The kidney total protein levels were significantly increased ($P \leq 0.005$) in the diabetic mice when compared to control group by 1.3-fold. The liver and kidney total protein increased significantly ($P \leq 0.0001$ and $P \leq 0.01$) upon vanadyl$(VO)^{2+}$/vit B6 complex treatment as compared to diabetic group.

Total protein in serum is synthesized exclusively by the liver. It is secreted from the Golgi apparatus across the sinusoidal membrane of the hepatocytes [97]. Total proteins were considered to be important in the maintenance of health. Reduction in liver total protein level was observed in diabetic mice. The reported results concerning the decrease in total proteins during diabetes agreed with those of Rawi et al. [3] who showed a decrease in total proteins

Table 13 The correlation (Pearson's test) among the biochemical parameters of serum in mice

Parameters	Glucose	TG	TC	HDL-c	LDL-c	VLDL-c	LDH	Uric acid	Creatinine	G6PD	RBCs	Hb	WBCs	Platelets
Glucose	1	0.753*	0.561	−0.985**	0.545	0.753*	0.686	−0.236	0.649	−0.627*	−0.627*	−0.422	0.128	0.626
TG	0.753*	1	0.779*	−0.828*	0.738*	1.0**	0.925**	−0.105	0.519	−0.573*	−0.699*	−0.603*	0.607*	0.679*
TC	0.561	0.779*	1	−0.673	0.998**	0.779*	0.729*	-0.520	0.712*	−0.859**	−0.794*	−0.901**	0.170	0.829*
HDL−c	−0.985**	−0.828*	−0.673	1	−0.656	−0.828*	−0.737*	0.316	−0.702	0.704	0.726*	0.534	−0.199	−0.697
LDL−c	0.545	0.738*	0.998**	−0.656	1	0.738*	0.689	−0.559	0.726*	−0.876**	−0.790*	−0.910**	0.108	0.830*
VLDL−c	0.753*	1.0**	0.779*	−0.828−*	0.738*	1	0.925**	−0.105	0.519	−0.573	−0.699	−0.603	0.607	0.679
LDH	0.686	0.925**	0.729*	−0.737−*	0.689	0.925**	1	0.079	0.462	−0.520	−0.515	−0.636	0.584	0.489
Uric acid	−0.236	−0.105	−0.520	0.316	−0.559	−0.105	0.079	1	−0.778*	0.671	0.695	0.474	0.470	−0.525
Creatinine	0.649	0.519	0.712*	−0.702	0.726*	0.519	0.462	−0.778*	1	−0.771*	−0.770*	−0.641	−0.208	0.573
G6PD	−0.627	−0.573	−0.859**	0.704	−0.876**	−0.573	−0.520	0.671	−0.771*	1	0.866**	0.809*	0.097	−0.710*
RBCs	−0.627	−0.699*	−0.794*	0.726*	−0.790*	−0.699	−0.515	0.695	−0.770*	0.866**	1	0.610	−0.124	−0.732*
HB	−0.422	−0.603	−0.901**	0.534	−0.910**	−0.603	−0.636	0.474	−0.641	0.809*	0.610	1	−0.152	−0.591
WBCs	0.128	0.607	0.170	−0.199	0.108	0.607	0.584	0.470	−0.208	0.097	−0.124	−0.152	1	−0.011
Platelets	0.626*	0.679*	0.829*	−0.697*	0.830*	0.679	0.489	−0.525	0.573	−0.710*	−0.732*	−0.591	−0.011	1

TG triglycerides, *TC* total cholesterol, *HDL-c* density lipoprotein-cholesterol, *LDL-c* low density lipoprotein-cholesterol, *VLDL* volatile low density lipoprotein-cholesterol, *LDH* lactic dehydrogenase, *G6PD* glucose 6- phosphate dehydrogenase, *RBCs* red blood cells, *Hb* hemoglobin and *WBCs* white blood cells

* Correlation is significant at the 0.05 level (2-tailed)

** Correlation is significant at the 0.01 level (2-tailed)

of liver and serum during diabetes. The decrease in protein may be due to microproteinuria and albuminuria, which are important clinical markers of diabetic nephropathy [98], and may be due to increased protein catabolism [29]. Treatment the diabetic mice with vanadyl$(VO)^{2+}$/vit B6 complex increased in total proteins in liver and kidney by 6.59- and 1.33-fold as compared to diabetic mice (Fig. 9). Oral injection aqueous extracts of *Phyllathus amarus, Vitex doniana* and *vitex doniana* (100 mg/kg) each alternative day for 21 days significant increase total proteins in liver tissues by 2.24-, 1.96- and 1.98- fold as compared to diabetic rat [99].

3.2.7.6 The correlation (Pearson's test) among the biochemical parameters of serum in mice Table 13 showed the correlation (Pearson's test) among the biochemical parameters of serum in mice. Glucose levels had positive correlation with TG and VLDL-c levels and had negative correlation with the level of HDL-c, activity of G6PD and number of RBCs. TG level had positive correlation with the levels of TC, LDL-c, VLDL-c, LDH as well as the number of WBCs and platelets and negative correlation with level of HDL-c, activity of G6PD, number of RBCs and Hb content. TC level had positive correlation with the levels of LDL-c, VLDL-c, LDH, creatinine and platelets number and had negative correlation with the activity of G6PD, number of RBCs and Hb content.

In conclusion, the results suggested that vanadyl$(VO)^{2+}$/vit B6 complex has an anti-diabetic potency and has ability to improve the lipid profile and the antioxidant activity.

References

1. Tanko Y, Yaro AH, Isa AI, Yerima M, Saleh MI, Mohammed A. Toxicological and hypoglycemic studies on the leaves of *Cissampelos mucronata (Menispermaceae)* on blood glucose levels of streptozotocin-induced diabetic wistar rats. J Med Plant Res. 2007;1((5)):113–6.
2. Bhat M, Kothiwale KS, Tirmale RA, Bhargava YS, Joshi NB. Antidiabetic Properties of *Azardiracta indica* and *Bougainvillea spectabilis* in vivo studies in murine diabetes model. Ins. Bioinform. Biotechnol. PubMed Central 3695 (2011) Records.
3. Rawi MS, Mourad MI, Sayed AD. Biochemical and changes in experimental diabetes before and after treatment with *Mangifera indica Psidium guava* extracts. Int J Pharm Biomed Sci. 2011;2(2):29–41.
4. Kang KS, Kim HY, Pyo JS, Yokozawa T. The effects of glycine and L-arginine on heat stability of ginsenoside. Biol Pharm Bull. 2006;29:750–4.
5. Ahmed N. Advanced glycation end products-role in pathology of diabetic complications. Diabetes Res Clin Pract. 2005;67:3–21.
6. Srivatsan R, Das S, Gadde R, Manoj-Kumar K, Taduri S, Rao N, Ramesh B, Baharani A, Shah K, Kamireddy SC, Priyatham G, Balakumaran TA, Seshadri A, Rao A. Antioxidants and lipid peroxidation status in diabetic patients with and without complications. Arch Iran Med. 2009;12(2):121–7.
7. American Diabetes Association. Diagnosis and classification of diabetes mellitus. Diabetes Care. 2011;31:55–60.
8. Guyton A, Hall J. Text book of medical physiology. Philadelphia: Elsevier; 2006. p. 836–9.
9. Oliveri M, Davio C, Alcira M, Batlle C, Gerez NE. ALAS-1 gene expression is down-regulated by Akt-mediated phosphorylation and nuclear exclusion of Foxoi by vanadate in diabetic mice. Biochem J Immed Pub. 2011;20(1):11–50.
10. Mukherjee B, Patra B, Mahapatra S, Banerjee P, Tiwari A, Chatterjee M. Vanadium an element of a typical biological significance. Toxicol Lett. 2004;150(2):135–43.
11. Zhang H, Yi Y, Feng D, Wang Y, Qin S. Hypoglycemic properties of oxovanadium (IV) coordination compounds with carboxymethyl-carrageenan and carboxymethyl-chitosan in alloxan-induced diabetic mice. Evidence Based Complement Altern Med. 2011;69(1):67–70.
12. Rodica-Mirela N, Lacatusu I, Badea N, Nichita C, Meghea A. Effect of vanadium on new silses quioxane-nano silica encapsulated bio-active compounds with potential for bio-medical application. UPB Sci Bull Ser B. 2011;73(2):1454–2331.
13. Crans DC, Smee JJ, Gaidamauskas E, Yang L. The chemistry and biochemistry of vanadium and the biological activities exerted by vanadium compounds. Chem Rev. 2004;104((2):849–902.
14. Srivastava AK, Mehdi MZ. Insulino-mimetic and anti-diabetic effects of vanadium compounds. Diabetes UK. Diabetes Med. 2004;22:2–13.
15. Refat SM, El-Shazly AS. Identification of a new anti-diabetic agent by combining VOSO4 and vitamin E in a single molecule Studies on its spectral, thermal and pharmacological properties. J Eur Med Chem. 2010;45:3070–9.
16. Hussain AM. The relationship between diabetes mellitus and periodontitis. Al Am En J Med Sci. 2011;4(1):84–6.
17. Xie M, Gao L, Li L, Li W, Yan S. A new orally active antidiabetic vanadyl complex bis(α-furancarboxylato) oxovanadium (IV). J Inorg Biochem. 2005;99:546–51.
18. Mukherjee T, Costa Pessoa J, Kumar A, Sarkar AR. An oxidovanadium(IV) schiff base complex derived from vitamin B6: synthesis, characterization and insulin enhancing properties. Inorg Chem. 2011;50(10):4349–61.
19. Revilla-Monsalve C, Zendejas-Ruiz I, Islas-Andrade S, Báez-Saldaña A, Palomino-Garibay MA, Hernández-Quiróz PM, Fernandez-Mejia C. Diabetic patients and in nondiabetic subjects with hypertriglyceridemia. Biomed Pharmacother. 2006;60:182–5.
20. Degenhardt TP, Alderson LN, Arrington DD, Beattie JR, Basgen MJ, Steffes WM, Thorpe RS, Baynes WJ. Pyridoxamine inhibits early renal disease and dyslipidemia in the streptozotocin-diabetic rat. Kidney Int. 2002;61:939–50.
21. MacKenzie KE, Wiltshire EJ, Gent R, Hirte C, Piotto L, Couper JJ. Folate and vitamin B6 rapidly normalize endothelial dysfunction in children with type 1 diabetes mellitus. Pediatrics. 2006;118(2):242–53.
22. Shriner A, Lippard SJ, Berg JM. Principles of bioinorganic chemistry. Mill Valley: University Science Books; 1997. p. 321–33.
23. Vogel A. Qualitative inorganic analysis. New York: Wiley; 1987.
24. Burger K, Fluck E, Binder H, Várhelyi CS. X-ray photoelectron spectroscopy (ESCA) investigations in coordination chemistry—II: the study of outer sphere coordination and hydrogen bridge formation in cobalt(III) and nickel(II) complexes. J Inorg Nucl Chem. 1975;37(1):55–7.
25. Abdullah M, Khairurrijal A. A simple method for determining surface porosity based on SEM images using origin pro software. Indonesian J Phys. 2009;20(2):37–40.
26. Sanford HS. Method for obtains venous blood from the orbital sinus of the rat or mouse. Science. 1954;119:100.

27. Edet EE, Akpanabiata MI, Ubon FE, Edet TE, Eno AE, Itam EH, Umon IB. *Gongronema latifolium* crude leaf extract reverses alterations in haemotological indices and weight loss in diabetic rats. J Pharm Toxicol. 2011;6(2):174–81.
28. Rerup CC. Drugs producing diabetes through damage of the insulin secreting cells. Pharmacol Rev. 1970;22:485–518.
29. Muruganandan S, Scrinivasan K, Gupta S, Gupta PK, Lal J. Effect of mangiferin on hyperglycemia and atherogenicity in streptozotocin diabetic rats. J Ethnopharmacol. 2005;97:497–501.
30. Prakasam A, Sethupathy S, Pugalendi KV. Hypolipidaemic effect of *Casearia esculenta* root extracts in streptozotocin-induced diabetic rats. Pharmazie. 2003;58(11):828–32.
31. Ohkawa H, Ohishi N, Yagi K. Assay for lipid peroxides in animal tissues by thiobarbituric acid reaction. Anal Biochem. 1979;95:351–8.
32. Rukmini MS, D'Souza B, D'Souza V. Superoxide dismutase and catalase activities and their correlation with malondialdehyde in Schizophrenic patients. Indian J Clin Biochem. 2004;19:114–8.
33. Habig WH, Pabst MJ, Jakoby WB. Glutathione-S-transferases: the first enzymatic step in mercapturic acid formation. J Biol Chem. 1974;249:7130–9.
34. Beutler E, Duron O, Kelly BM. Improved method for the determination of blood glutathione. J Lab Clin Med. 1963;61:882–8.
35. Prieto P, Pineda M, Aguilar M. Spectrophotometric quantitation of antioxidant capacity through the formation of a Phosphomolybdenum complex specific application to the determination of vitamin E. Anal Biochem. 1999;269:337–41.
36. Josephson B, Gyllensward CS. Colorimetric determination of total protein. J Clin Lab Invest. 1975;9:29–31.
37. El-Ezaby MS, El-Eziri FR. Equilibrium studies of some divalent metal ions complexes with pyridoxol, pyridoxal and pyridoxamine. J Inorg Nucl Chem. 1976;38:1901–5.
38. El-Ezaby MS, Rashad M, Moussa NM. Complexes of vitamin B6 polarographic determination of the stability constants of cadmium and zinc complexes with pyridoxamine. J Inorg Nucl Chem. 1977;39:175–7.
39. El-Dessouky MA, El-Ezaby MS, Abu Soud H. Complexes of vitamin B6. XVI. Kinetics and reaction mechanism of iron(III) complexes with pyridoxal-5-phosphate. Inorganica Chimica Acta. 1985;106(2):59–63.
40. Refat. MS. Synthesis and characterization of norfloxacin-transition metal complexes (group 11, IB): spectroscopic, thermal, kinetic measurements and biological activity. Spectrochimica Acta Part A. 2007;68:1393–405.
41. El-Dessouky MA, El-Ezaby MS, Abu Soud H. Complexes of vitamin B6. XVI. Kinetics and reaction mechanism of iron(III) complexes with pyridoxal-5-phosphate. Inorganica Chimica Acta. 1985;106(2):59–63.
42. George WO, Mcintyre PS. Infrared spectroscopy. Analytical chemistry by open learning. London: Wiley; 1987.
43. Singh HL, Vershney AK. "Synthetic, structural, and biochemical studies of organotin(IV) with Schiff bases having nitrogen and sulphur donor ligands. Bioinorg Chem Appl. 2006;2006:1–7.
44. Ozturk OF, Sekerci M, Ozdemir E. Synthesis of 5,6-O-Cyclohexylidene-1-amino-3-azahexane and Its Co(II), Ni(II), Cu(II) Complexes. Russ J Coord Chem. 2005;31:687–91.
45. Lever ABP. The electronic spectra of tetragonal metal complexes analysis and significant. Coord Chem Rev. 1968;3:119–40.
46. Garribba E, Micera G, Panzanelli A, Sanna D. Electronic structure of oxovanadium IV complexes of alpha-hydroxycarboxylic acids. Inorg Chem. 2003;42:3981–7.
47. Quan CX, Bin LH, Bang GG. Preparation of nanometer crystalline TiO_2 with high photo-catalytic activity by pyrolysis of titanyl organic compounds and photo-catalytic mechanism. Mater Chem Phys. 2005;91:317–24.
48. Osman AH, Aly AAM, Abd M, El-Mottaleb GAH. Gouda photoreactivity and thermogravimetry of copper(II) complexes of n-salicylideneaniline and its derivatives bull. Korean Chem Soc. 2004;25(1):45–50.
49. Refat MS, Killa HMA, El-Maghraby A, El-Sayed MY. Spectroscopic and thermal studies of perylene charge-transfer complexes. Bulgarian Chem Communica. 2012;44(1):74–82.
50. El-Awad AM. Catalytic effect of some chromites on the thermal decomposition of $KClO_4$ mechanistic and non-isothermal kinetic studies. J Therm Anal Calorim. 2000;61:197–208.
51. Singh G, Felix SP, Pandey DK. Studies on energetic compounds part 37: kinetics of thermal decomposition of perchlorate complexes of some transition metals with ethylenediamine. Thermochimica Acta. 2004;411:61–71.
52. Shinde NS, Dhadke NV, Suryakar NA. Evaluation of oxidative stress in type 2 diabetes mellitus and follow-up along with vitamin E supplementation. Indian J Clin Biochem. 2011;26(1):74–7.
53. Ravi K, Ramachandran B, Subramanian S. Protective effect of *Eugenia jambolana* seed kernel on tissue antioxidants in streptozotocin induced diabetic rats. Biol Pharma Bull. 2004;27:1212–7.
54. Ravi K, Rajasekaran S, Subramanian S. Antihyperlipidemic effect of *Eugenia jambolana* seed kernel on streptozotocin-induced diabetes in rats. Food Chem Toxicol. 2005;43:1433–9.
55. Tunali S, Yanardag R. Effect of vanadyl sulfate on the status of lipid parameters and on stomach and spleen tissues of streptozotocin-induced diabetic rats. Pharm Res. 2006;53:271–7.
56. Mahesar H, Bhutto MA, Khand AA, Narejo NT. Garlic used as an alternative medicine to control diabetic mellitus in alloxan induced male rabbits. Pak J Physiol. 2010;6(1):39–41.
57. Koyuturk M, Tunal S, Bolkent S, Yanardag R. Effects of vanadyl sulfate on liver of streptozotocin-induced diabetic rats. Biol Trace Elem Res. 2005;104:233–47.
58. Yanardag R, Demirci BT, seven UB, Bolkent S, Tunali S, Bolkent S. Synthesis, characterization and antidiabetic properties of N1-2,4-dihydroxybenzylidene-N4-2-hydroxybenzylidene-S-methylthiosemi-carbazidato-oxovanadium(IV). Eur J Med Chem. 2009;44:818–26.
59. Bolkent S, Bolkent S, Yanardag R, Tunali S. Protective effect of vanadyl sulphate on the pancreas of streptozotocin-induced diabetic rats. Diabetes Res Clin Pract. 2005;70:103–9.
60. Akgun-Dar K, Bolkent S, Yanardag R, Tunali S. Vanadyl sulfate protects against streptozotocin induced morphological and biochemical changes in rat aorta. Cell Biochem Funct. 2007;25:603–9.
61. Niu Y, Liu W, Tian C, Xie M, Gao L, Chen Z, Chen X, Li L. Effects of bis(α- furancarboxylato) oxovanadium(IV) on glucose metabolism in fat-fed/streptozotocin-diabetic rats. Eur J Pharmacol. 2007;572:213–9.
62. Sellamuthu SP, Muniappan PB, Perumal MS, Kandasamy M. Antihyperglycemic effect of mangiferin in streptozotocin induced diabetic rats. J Health Sci. 2009;55(2):206–14.
63. Rao G, Kamath U, Raghothama C, Pradeep KS. Maternal and fetal indicators of oxidative stress in various obstetric complications. Indian J Clin Biochem. 2003;18:80–6.
64. Comazzi S, Spagnolo V, Bonfanti U. Erythrocyte changes in canine diabetes mellitus: in vitro effects of hyperglycaemia and ketoacidosis. J Comp Clin Path. 2004;12:199–205.
65. Szudelski T. The mechanism of alloxan and streptozotocin action in ß cells of the rat pancreas. Physiol Res. 2001;50:536–46.
66. Kolanjiappan K, Manoharan S, Kayalvizhi M. Measurement of erythrocytes lipids, lipid peroxidation, antioxidants and osmotic fragility in cervical cancer patients. Clin Chim Acta. 2002;326:143–9.
67. Wu D, Cederbaum I. Alcohol, oxidative stress and free radical damage. Alcohol Res Health. 2003;27:277–84.
68. Vericel E, Januel C, Carreras M, Moulin P, Lagarde M. Diabetic patients without vascular complications display enhanced basal

platelet activation and decreased antioxidant status. Diabetes. 2004;53:1046–51.
69. Queen LR, Ji Y, Goubareva I, Ferro A. Nitric oxide generation mediated by beta-adrenoceptors is impaired in platelets from patients with type II diabetes mellitus. Diabetologia. 2003;46: 1474–82.
70. Fatini C, Sticchi E, Bolli P, Marcucci R, Giusti B, Paniccia R, Gori AM, Gensini GF, Abbate R. Platelet aggregability is modulated by eNOS locus in non-type 2 diabetic patients with acute coronary syndrome. Nutr Metab Cardiovasc Dis. 2011;21(1): 11–7.
71. Varughese G, Tomson J, Lip G. Type 2 diabetes mellitus: a cardiovascular perspective. Int J Clin Pract. 2005;59:798–816.
72. Zeinab AR. The effects of antioxidants supplementation on haemostatic parameters and lipid profiles in diabetic rats. J Am Sci. 2011;7(3):835–40.
73. Sy GY, Nongomierm RB, Sarr M, Cisse A, Fage B. Antidiabetic activity of the leaves of *Vernonia colorata* (wilid.) Draka (Composes) in alloxan induced diabetic rat. Dakar. Med. 2004; 49:36–9.
74. Pari L, Satheesh MA. Antidiabetic activity of *Boerhaavia diffusa* L effect on hepatic key enzymes in experimental diabetes. J Pharmacol. 2004;91(1):109–13.
75. Rajasekaran S, Sriram N, Arulselvan P, Subramanian S. Effect of aloe vera leaf gel extract on membrane bound phosphatases and lysosomal hydrolases in rats with streptozotocin. Diabetes. 2006;62(3):221–5.
76. Pushparaj P, Tan C, Tan B. Effects of *Averrhoe bilimli* leaf extract on blood glucose and lipids in streptozotocin diabetic rats. J Ethnopharmacol. 2000;72:69–76.
77. Gupta D, Raju J, Prakash JR, Baquer NZ. Change in the lipid profile, lipogenic and related enzymes in the livers of experimental diabetic rats effect of insulin and vanadate. Diabetes Res Clin Pract. 1999;46:1–7.
78. Eddouks M, Lemhadri A, Michel JB. Hypolipidemic activity of aqueous extract of *Capparis spinosa* L. in normal and diabetic rats. J Ethnopharmacol. 2005;98:345–50.
79. Sharma SB, Nasir A, Prabhu KM, Murthy PS, Dev G. Hypoglycaemic and hypolipidemic effect of ethanolic extract of seeds of *Eugenia jambolana* in alloxan-induced diabetic rabbits. J Ethnopharm. 2003;85:201–6.
80. Slater HL, Packard CJ, Bicker S, Shephered J. Effects of cholestyramine on receptor mediated plasma clearance and tissue uptake of human low density lipoprotein in the rabbit. J Biol Chem. 1980;255:10210–3.
81. Khanna K, Rizvi F, Chander R. Lipid lowering activity of *Phyllanthus niruri* in hyperlipidemic rats. J Ethnopharmacol. 2002;82:19–22.
82. Otamere HO, Aloamaka CP, Okokhere PO, Adisa WA. Lipid profile in diabetes mellitus what impact has age and duration. Br J Pharmacol Toxicol. 2011;2(3):135–7.
83. Karthik D, Ravikumar S. Proteome and phytochemical analysis of Cynodon dactylon leaves extract and its biological activity in diabetic rats. Biomed Pharmacother. 2010;10:9–19.
84. Zhang J, Steele M, Schweiger A. Arctic sea ice response to atmospheric forcings with varying levels of anthropogenic warming and climate variability. Geophys Res lett. 2010;37:205.
85. Ugochukwu NH, Babady NE. Antihyperglycemic effect of aqueous and ethanolic extracts of *Gongronema latifolium* leaves on glucose and glycogen metabolism in livers of normal and streptozotocin-induced diabetic rats. Life Sci. 2003;73:1925–38.
86. Gad ZM, Ehssan AN, Ghiet HM, Wahman FL. Effects of pioglitazone and metformin on carbohydrate metabolism in experimental models of glucose intolerance. Int J Diabetes Metab. 2010;18:132–8.
87. Gawronska-Szklarz B, Musial D, Pawlik A, Paprota B. Effect of experimental diabetes on pharmacokinetic parameters of lidocaine and MEGX in rats. Poll J Pharmacol. 2003;55:619–24.
88. Ashakiran S, Krishnamurthy N, Navin S, Patil S. Behaviour of serum uric acid and lipid profile in relation to glycemic status in proliferative and non-proliferative diabetic retinopathy. Curr Neurobiol. 2010;2(1):57–61.
89. Zari AT, AL-Logmani A. Long-term effects of Cinnamomum zeylanicum Blume oil on some physiological parameters in streptozotocin-diabetic and non- diabetic rats. Boletín Latinoamericano y del Caribe de Plantas Medicinales y Aromáticas. 2009;8(4):266–74.
90. Ganong W. Review of medical physiology, Lange medical books, vol. 13. New York: McGraw-Hill; 2003. p. 912–78.
91. Sh. AL-Logmani A, Zari TA. Effects of *Nigella sativa* L. and *Cinnamomum zeylanicum* blume oils on some physiological parameters in streptozotocin-induced diabetic rats. Boletín Latinoamericano y del Caribe de Plantas Medicinales y Aromáticas. 2009;8(2):86–96.
92. Rajeshwari CU, Andallu B. Oxidative stress in NIDDM patients influence of coriander (*Coriandrum sativum*) seeds. Res J Pharm Biol Chem Sci. 2011;2(31):0975–8585.
93. Rajasekaran S, Sivagnanam K, Subramanian S. Mineral contents of *Aloe vera* leaf gel and their role on streptozotocin-induced diabetic rats. Pharmacology. 2005;57:185–95.
94. Pourkhalili N, Hosseini A, Nili-Ahmadabadi A, Hassani S, Pakzad M, Baeeri M, Mohammadirad A, Mohammad A. Biochemical and cellular evidence of the benefit of a combination of cerium oxide nanoparticles and selenium to diabetic rats. World J Diabetes. 2011;2(11):204–10.
95. Hayes JD, Flanagan JU, Jowsey IR. Glutathione transferases. Ann Rev Pharmacol Toxicol. 2005;45:51–88.
96. Velladath US, Asha D, Rishikesh K, Nalini K. Erythrocyte glutathione-S-transferase activity in diabetics and its association with HBA1c. Webmed Cent Clin Biochem. 2011;2(7): 1690–2046.
97. Suchetha-Kumari N, Sathyavathi A, Paramesha S, Damodara Gowda KM, Mahesh K. Combined effect of aqueous extracts of *Phyllathus amarus* and *Vitex doniana* stem bark on blood glucose of streptozotocin (stz) induced diabetes rats and some liver biochemical parameters. Int J Appl Biol Pharm Technol. 2011; 2:0976–4550.
98. Leiro JM, Alvarez E, Arranz JA, Siso IG, Orallo F. In vitro effects of mangiferin on superoxide concentrations and expression of the inducible nitric oxide synthase, tumor necrosis factor and transforming growth factor genes. Biochem Pharmacol. 2003; 65:1361–71.
99. Owolabi OA, James DB, Anigo KM, Iormanger GW, Olaiya II. Combined effect of aqueous extracts of *Phyllathus amarus* and *Vitex doniana* stem bark on blood glucose of streptozotocin (STZ) induced diabetes rats and some liver biochemical parameters. Br J Pharmacol Toxicol. 2011;2(3):143–7.